9-2019

The Role of Autophagy in Myocardial Ischemia/Reperfusion Injury in Isolated Rat Hearts

Aloysius C. Ibe II
Philadelphia College of Osteopathic Medicine

Philadelphia College of Osteopathic Medicine

School of Health Sciences

Graduate Program in Biomedical Sciences

The Role of Autophagy in Myocardial Ischemia/Reperfusion Injury in Isolated Rat Hearts

A Thesis in Biomedical Sciences by Aloysius C. Ibe,II

Submitted in Partial Fulfillment of the Requirements for the Degree of Masters in Biomedical Sciences

September 2019

This thesis has been presented to and accepted by the Associate Dean for Curriculum and Research Office of Philadelphia College of Osteopathic Medicine in partial fulfillment of the requirements for the degree of Master of Science in Biomedical Sciences.

We, the undersigned, duly appointed committee have read and examined this manuscript and certify it is adequate in scope and quality as a thesis for this master's degree. We approve the content of the thesis to be submitted for processing and acceptance.

_____

Qian Chen, Ph.D, Thesis Advisor
Assistant Professor of Physiology and Pharmacology
Department of Bio-Medical Sciences

_____

Dawn Shell, Ph.D, Thesis Committee Member
Associate Professor of Microbiology and Immunology
Department of Bio-Medical Sciences

_____

Charlotte Greene, Ph.D, Thesis Committee Member
Professor of Physiology
Department of Bio-Medical Sciences

_____

Marcus Bell, Ph.D., Program Director, Research Concentration
Master of Science in Biomedical Sciences
Professor
Department of Bio-Medical Sciences

ABSTRACT

Autophagy is a housekeeping process used to remove damaged cytoplasmic constituents and protein aggregates. However, a debate persists on whether autophagy is beneficial or detrimental when an ischemic/reperfusion (I/R) insult occurs in the heart. This study tested the effects of autophagy enhancers (rapamycin and trehalose) and an autophagy inhibitor (3-methyladenine) on cardiac function and infarct size after global ischemia (30 minutes) and reperfusion (45 minutes) when given prior to ischemia (pre-treatment) or at the beginning of reperfusion (post-treatment). Rapamycin (25nM) pre-treatment and post-treatment significantly restored final left ventricular developed pressure (LVDP) to 75.4±9.1% and 60±5% of initial baseline respectively (both n=5, $p<0.05$), compared to control I/R group (n=9) that recovered to 35±5.5% of initial baseline. Likewise, trehalose (5mM) pre-treatment and post-treatment also significantly restored final LVDP to 61.4±3.7% (n=6) and 69.1±2.7% (n=5) of their initial baseline respectively, compared to control I/R group ($p<0.05$). However, 3-Methyladenine (1mM) pre-treatment (n=6) and post-treatment (n=5) showed similar reduction in final LVDP to 24.7±9.1% and 33.4±12.8 % of their initial baseline respectively, as the control I/R group. Moreover, infarction percentage was significantly reduced by rapamycin pre-treatment and post-treatment (14 ± 2.8% and 21.4 ± 5.3%, respectively; both $p<0.05$); and trehalose pre-treatment and post-treatment (19.2 ± 3% and 15.2% ± 3, respectively; both $p<0.05$), but not by 3-Methyladenine pre-treatment or post-treatment (26±2% and 28±4.1%, respectively) when compared to control I/R group (38.6±4.3%). The data suggests that autophagy enhancement before ischemia or at reperfusion reduces I/R injury.

TABLE OF CONTENTS

LIST OF FIGURES

ACKNOWLEDGEMENTS

Research Committee

Qian Chen PhD

Charlotte Greene PhD

Dawn Shell PhD

Biomedical Science and Work-study students

Anahi McIntyre, Robinder Sandhu, and Dylan Lefkowitz

Alisa Kim and Marquese Daniels

We would also like to thank PCOM faculty member Lindon Young PhD and PCOM alumni

Andrew Castellano.

Director of Biomedical Sciences

Marcus Bell PhD

This study was supported by the Division of Research, Center for Chronic Diseases of Aging, and the Department of Biomedical Sciences at the Philadelphia College of Osteopathic Medicine (PCOM).

INTRODUCTION

Cardiovascular disease (CVD) is the number-one cause of death globally. As of 2016 an estimated 85.6 million American adults suffer from some type of CVD accounting for 1 of every 3 deaths in the United States (AHA, 2016) (Mozaffarian, 2015). Individuals who are at a higher risk of CVD include those who heavily use tobacco, have a poor diet, or are physically inactive (AHA, 2016). African Americans, as well as Non-Hispanic Whites, have the highest likelihood of suffering from CVD, followed by Alaskan Natives and Asians (CDC, 2016). Normally, the heart pumps blood into the systemic circulation and it is the blood that carries oxygen and nutrients to other organ systems within the body, thus allowing the organs systems to perform their function properly.

1.1 Cardiac Physiology

The heart perfuses itself with blood, nutrients, and oxygen via its coronary arteries and acts as a pump by sending blood to all the organ systems through pulmonary and systemic circulations (Klabunde, 2016). The coronary artery originates from the aorta and splits into two vessels, providing blood to each side of the heart (Rice University, 2012). The left coronary artery supplies blood to the left atrium, left ventricle, and interventricular septum while the right coronary artery supplies blood to the right atrium, both portions of the ventricles, and the heart's electrical conduction system (Rice University, 2012). The coronary arteries from both sides of the heart branch to form smaller arteries that eventually anastomose, providing blood to sustain the heart muscle. An anastomosis is "an area where vessels unite to form interconnections that

normally allow blood to circulate to a region even if there may be partial blockage in another branch" (Rice University, 2012).

The heart is a four-chambered pump that functions to circulate blood throughout the body by a rhythmical contraction and relaxation of its muscular walls. Rhythmical activity is controlled by an intrinsic electrical conduction system that is regulated by extrinsic autonomic nerves. Deoxygenated blood is returned to the right side of the heart which then delivers it to the lungs where oxygen is absorbed, and carbon dioxide removed. Oxygenated blood leaves the lungs and enters the left side of the heart where it is then propelled into the systemic circulation.

1.2 Cardiac Anatomy

The four chambers of the heart are the right atrium (RA), right ventricle (RV), left atrium (LA), and left ventricle (LV). The right and left side of the heart are separated by a thick septum and the atrium and ventricles are separated by the atrioventricular valves. Specifically, the RA and RV are separated by the tricuspid valve while the LA and LV are separated by the mitral/bicuspid valve. The valves that lead to pulmonary and systemic circulation are collectively known as the semilunar valves (Argosy, 2018). The pathway from the RV leads to the pulmonary valve, then into the pulmonary circulation while the LV pathway leads to the aortic valve then into systemic circulation. The function of all these valves is to permit unidirectional blood flow in the heart by preventing backflow of blood.

1.2.1 The Cardiac Cycle

Normal blood flow through the heart is as follows: (Figure 1)

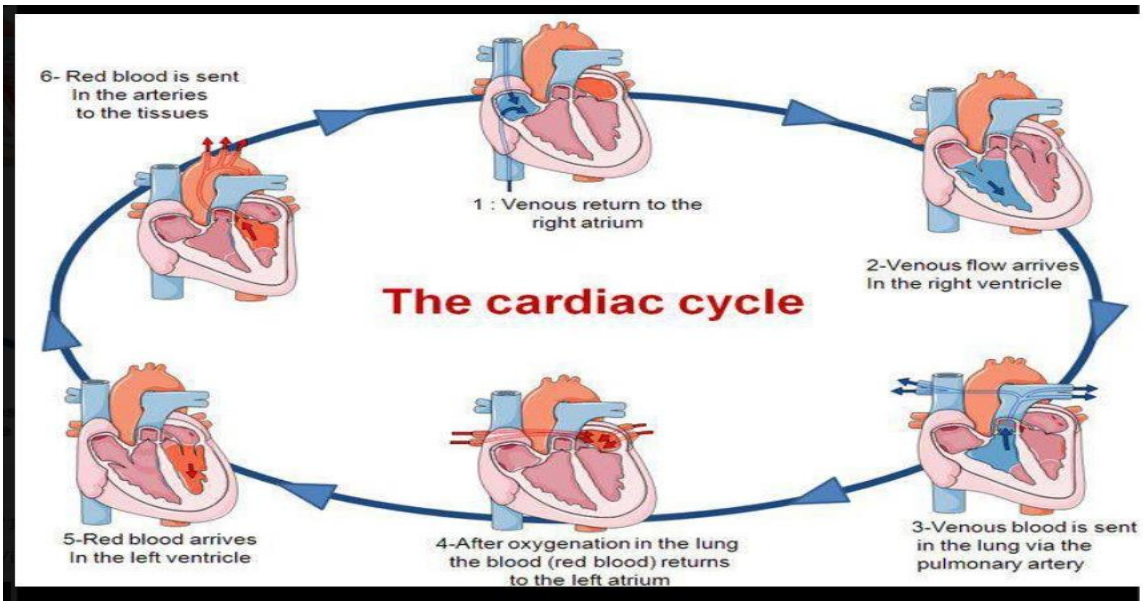

Figure 1. The Cardiac Cycle

The right and left sides of the heart function simultaneously to expel the same volume of blood. Both the right and left atria fill passively (atrial diastole). Once ventricular pressure falls below atrial pressure, the mitral and tricuspid valves open and ventricular filling begins (ventricular diastole). The atria then contract (atrial systole). When the pressure in the ventricles rises above the pressure in the atria, the mitral and tricuspid valves close. Contraction of the ventricle follows, which causes ventricular forces to open the semilunar valves allowing the ventricles to empty their contents into the pulmonary and systemic circulations.

1.2.2 Cardiac Muscle Excitation-Contraction Mechanism

Cardiac muscle does not only consist of muscular tissue, but connective tissue as well that holds contractile cells together in bundles known as fascicles and allows for flexibility. Within the fascicles are myofibers and the proteins actin and myosin that actually allow for

muscle contraction and relaxation. Microscopically, actin is seen as thin filaments while myosin is seen as thick filaments that have a tail and head component. Actin and myosin overlap each other and collectively appear as striations known as sarcomeres.

A myofibril has many sarcomeres that are separated by Z-lines. Actin (thin filaments) are attached to the Z-lines and overlap with myosin (thick filaments) in the middle of each sarcomere, known as the A-band region, where contraction occurs when the thin and thick filaments slide past each other. Myosin is not directly attached to the Z-lines. Within the sarcomere the region where thick filaments are found exclusively is called the H-zone while the I-band is the only area where thin filaments are found by themselves (Figure 2).

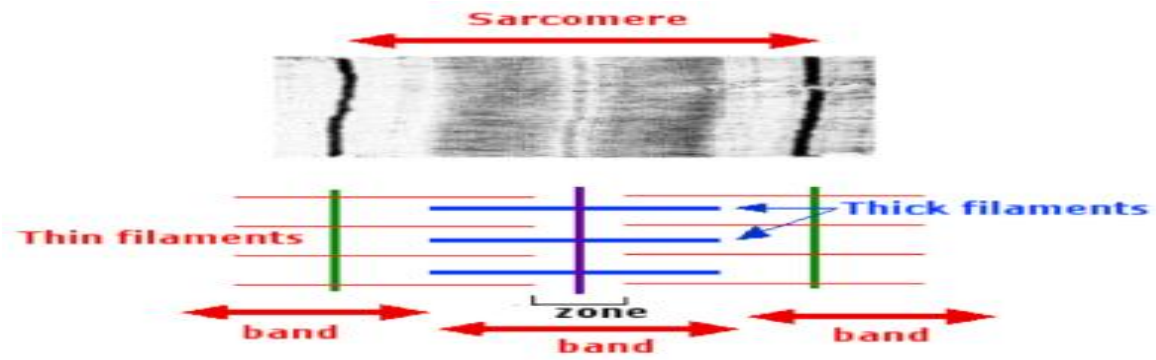

Figure 2. Sarcomere structure

When the actin and myosin slide past each other muscle contraction occurs, bringing the Z-lines closer to each other, and shortening the muscle. This sliding process is powered by ATP. The myosin head attaches to the myosin binding site on an actin molecule to form a “cross bridge.” The steps of contraction are as follows: cross bridge formation (where myosin is bound by ADP and Pi), power stroke (myosin pulls the actin toward the center of the sarcomere and

ADP is released), binding of new ATP to release cross bridge (i.e. relaxation), and finally ATP hydrolysis so the cycle can repeat itself once myosin binds to a new site.

The contractile steps occur spontaneously, but calcium is required for contraction because the troponin-tropomyosin complex prevents contraction when calcium is absent. Tropomyosin is a fibrous protein that blocks the myosin binding sites, thus preventing cross bridge formation. Troponin is a globular protein attached to tropomyosin and can bind to calcium. Once troponin binds to calcium it moves tropomyosin in such a manner that the myosin binding site will be free to interact with actin for cross bridge formation and allow for contraction. The source of calcium used in this process is found intracellularly in the sarcoplasmic reticulum or from the extracellular fluid. The calcium not only permits the excitation-contraction mechanism, but also is involved in the function of the electrical conduction system of the heart once an action potential is generated.

1.2.3 Electrical Conduction System and Action Potentials of the Heart

In order for the heart to contract, an action potential must occur, causing the cardiac muscle to depolarize and ultimately pass the wave of depolarization is carried throughout the entire heart. Cardiac muscle tissue has autorhythmicity, meaning that is has the ability to generate an action potential without the need of outside stimulation (Rice University, 2012). The two types of cardiac muscle cells are: myocardial contracting cells (i.e., cardiomyocytes) and myocardial conducting cells. The cardiomyocytes make up the majority of the cells found in both the atria and ventricles while the conducting cells account for only 1% of the cells found in the atria and ventricles and is responsible for the autorhythmicity of the heart (Rice University, 2012).

The conducting cells consist of the sinoatrial (SA) node, atrioventricular (AV) node, bundle of His, and Purkinje fibers, and the electrical conduction system occurs in that order (Figure 3). Normal cardiac rhythm is established by the SA node because it has the highest rate of depolarization, meaning that it is the first conducting cell to fire an action potential (Rice University, 2012). Since it is the first to fire an action potential the SA node serves as the "pacemaker" for the heart.

Although each part of the conduction system can generate its own impulse, the rate of depolarization progressively slows from the SA node onwards. For example, if the SA node is damaged, the AV node takes over as the "new" pacemaker, even though the conduction occurs at a slower rate, because the AV node has the second fastest rate of depolarization.

The normal cardiac rhythm is influenced by the sympathetic and parasympathetic branches of the autonomic nervous system. The sympathetic nervous system increases the rate of depolarization of the SA node, and ultimately the heart rate. The parasympathetic nervous system, decreases the rate of depolarization of the SA node and ultimately the heart rate.

Once an action potential is generated, the electrical signal spreads from the SA node to the AV node via internodal pathways. The AV node is located on the inferior portion of the right atrium. A slight pause in the conduction occurs before the AV node depolarizes and sends the electrical signal farther down the conduction pathway. This pause allows the atria to complete their emptying of blood into the ventricle before the signal reaches the ventricle itself (Rice University, 2012).

The bundle of His and the Purkinje fibers continue the pathway of depolarization, which spreads the electrical signal throughout the ventricles. The contraction of the ventricles expels

blood into the pulmonary artery or aorta by the right or left ventricle, respectively. The conduction time from the SA node to the Purkinje Fibers is approximately 225ms (Rice University, 2012) (Figure 3).

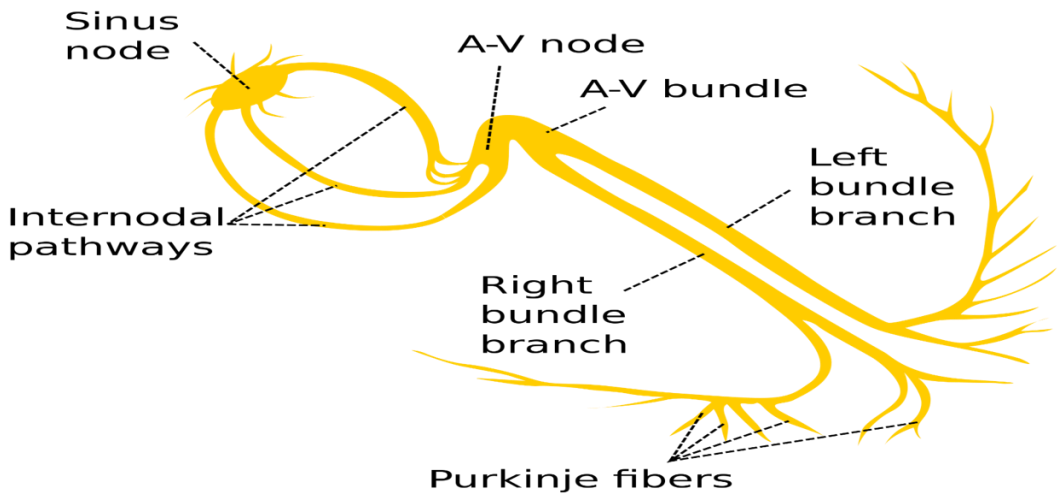

Figure 3. Electrical Conduction Pathway of the Heart

1.3 Calcium in Cardiac Muscle

Both the cardiac contracting and conducting cell membranes can be depolarized; however, the way in which the membrane potential is reached, and the ion movement occurs is different. Sodium (Na+) and potassium (K+) are required for depolarization and repolarization of an action potential respectively, however, Ca2+ is required for both contracting and conducting cell depolarization (Rice University, 2012).

1.3.1 Conducting Cells

Cardiac conducting cells do not have a stable resting membrane potential (RMP). Instead, they spontaneously depolarize. Slow, open Na+ channels cause the membrane potential to rise from an initial value of -60mV to -40mV. This spontaneous depolarization accounts for the autorhythmicity of cardiac muscle (Rice University, 2012). Once the membrane potential reaches -40mV, Ca2+ channels open and induce depolarization until a value of +5mV is reached. At the peak of membrane voltage (+5mV), Ca2+ channels close and K+ channels open, allowing K+ to exit and repolarize the cell back to its initial value (Rice University, 2012). See Figure 4.

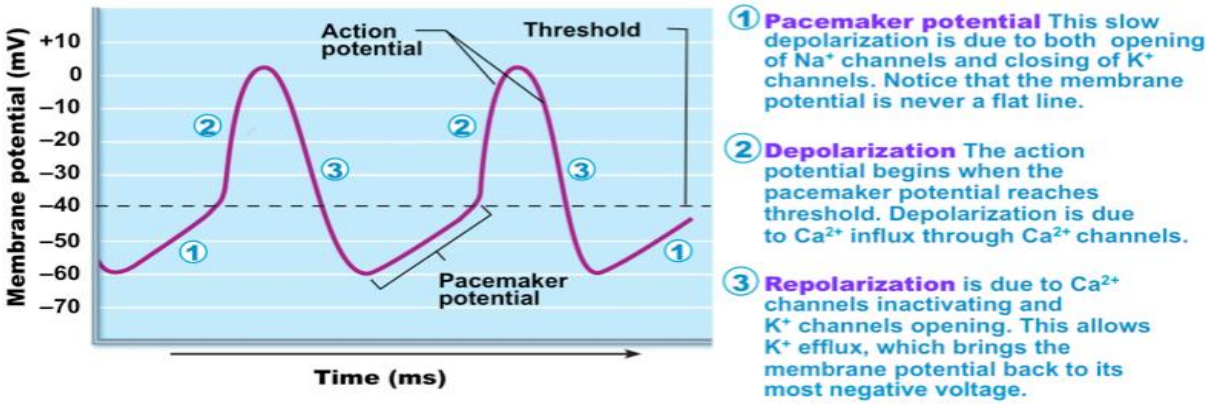

Figure 4. Action Potential in Conducting Cells

1.3.2 Contracting Cells

The electrical pattern for contracting cells is different in that the resting membrane potential is stable, depolarization is rapid, and depolarization is followed by a plateau phase (Rice University, 2012). The plateau phase accounts for the relatively long refractory period in cardiac-muscle cells. A refractory period is a time where the muscle will not respond to a

stimulus. This long refractory period allows the cardiac muscle to pump blood effectively before the cardiac muscle cells fire an action potential for a second time. The steps involved in the development of an action potential are as follows: initial resting membrane potential of -90mV to -80mV. Once threshold is reached, Na+ channels open, and an inflow of Na+ occurs until approximately +25mV is reached. Once the peak voltage has been met, Na+ channels close; however, Ca2+ channels open and account for the plateau phase and relatively slow rate of membrane potential decline (Rice University, 2012). After the membrane potential declines to 0mV, Ca2+ channels close, K+ channels open, and K+ exits the cell allowing for repolarization of the membrane. The membrane continues to drop until it reaches its initial values, K+ channels close, and the cycle repeats itself. The entire cycle lasts 250 to 300ms (Rice University, 2012) (Figure 5).

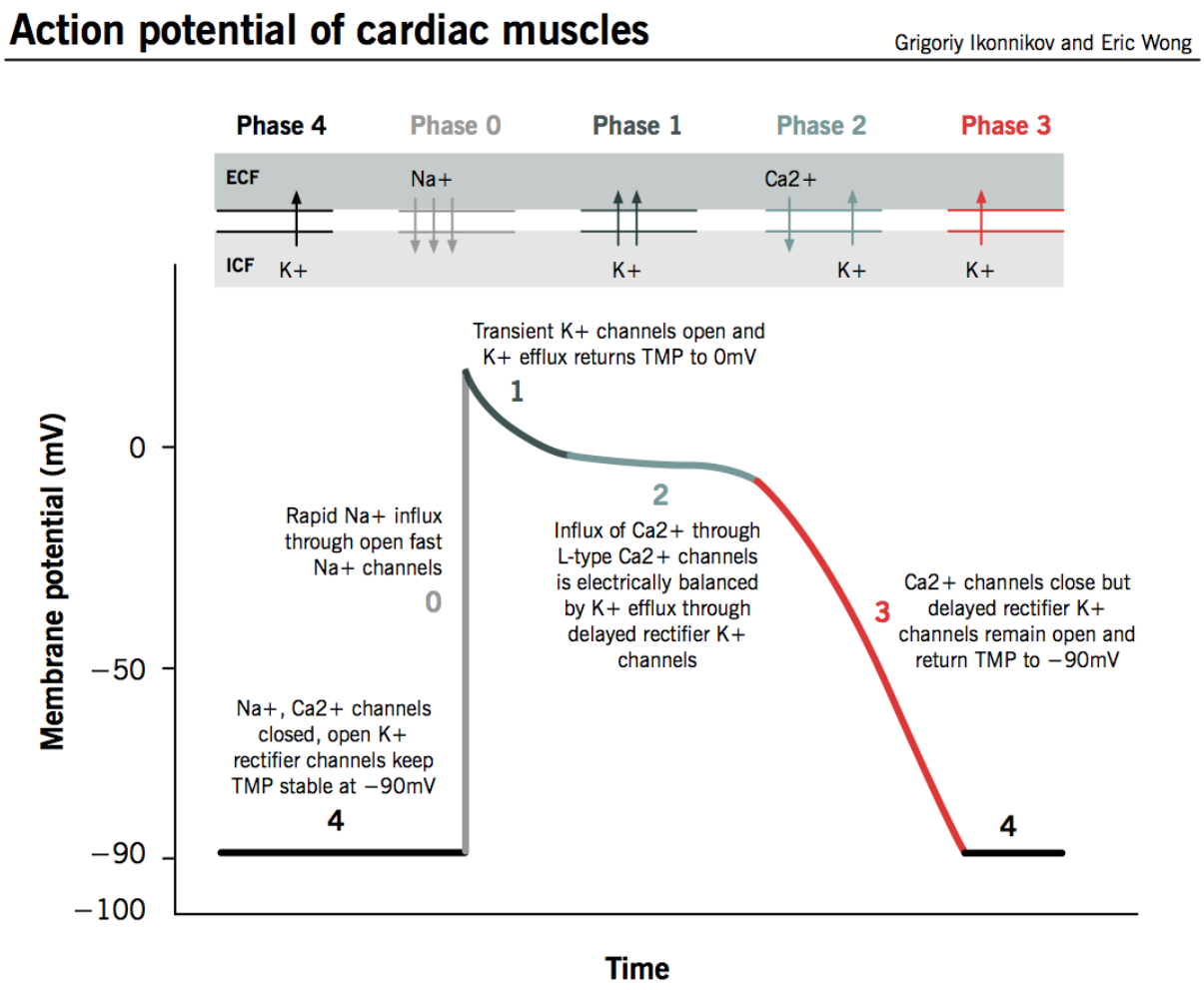

Figure 5. Action Potential in Contracting Cells

Therefore, the importance of the Ca2+ is twofold: (1) Ca2+ is involved in the troponin-tropomyosin complex that initiates the mechanical contraction of the heart (i.e., excitation contraction coupling) and (2) it accounts for the plateau phase of the action potential. However, in order for this to occur cardiac function is dependent upon an adequate source of energy.

1.4 Cardiac Muscle Metabolism

The heart has the highest metabolic demand of any organ system in the body. More than 95% of ATP generated in the heart is derived from oxidative phosphorylation in the mitochondria. The remaining 5% comes mainly from glycolysis and to a lesser extent from the citric acid cycle (Krebs cycle) (Ingwall, 2009).

Substrates are transported across the extracellular membrane into the cytosol and are metabolized in various ways. For oxidation, the respective metabolic intermediates (e.g., pyruvate or acyl-coenzyme A [CoA]) are transported across the inner mitochondrial membrane by specific transport systems. Once inside the mitochondrion, substrates are oxidized or carboxylated (anaplerosis) and fed into the Krebs cycle for the generation of reducing equivalents (reduced nicotinamide adenine dinucleotide [NADH]2; reduced flavin adenine dinucleotide [FADH]) and GTP. The reducing equivalents are used by the electron transport chain to generate a proton gradient, which in turn is used for the production of ATP (Figure 6).

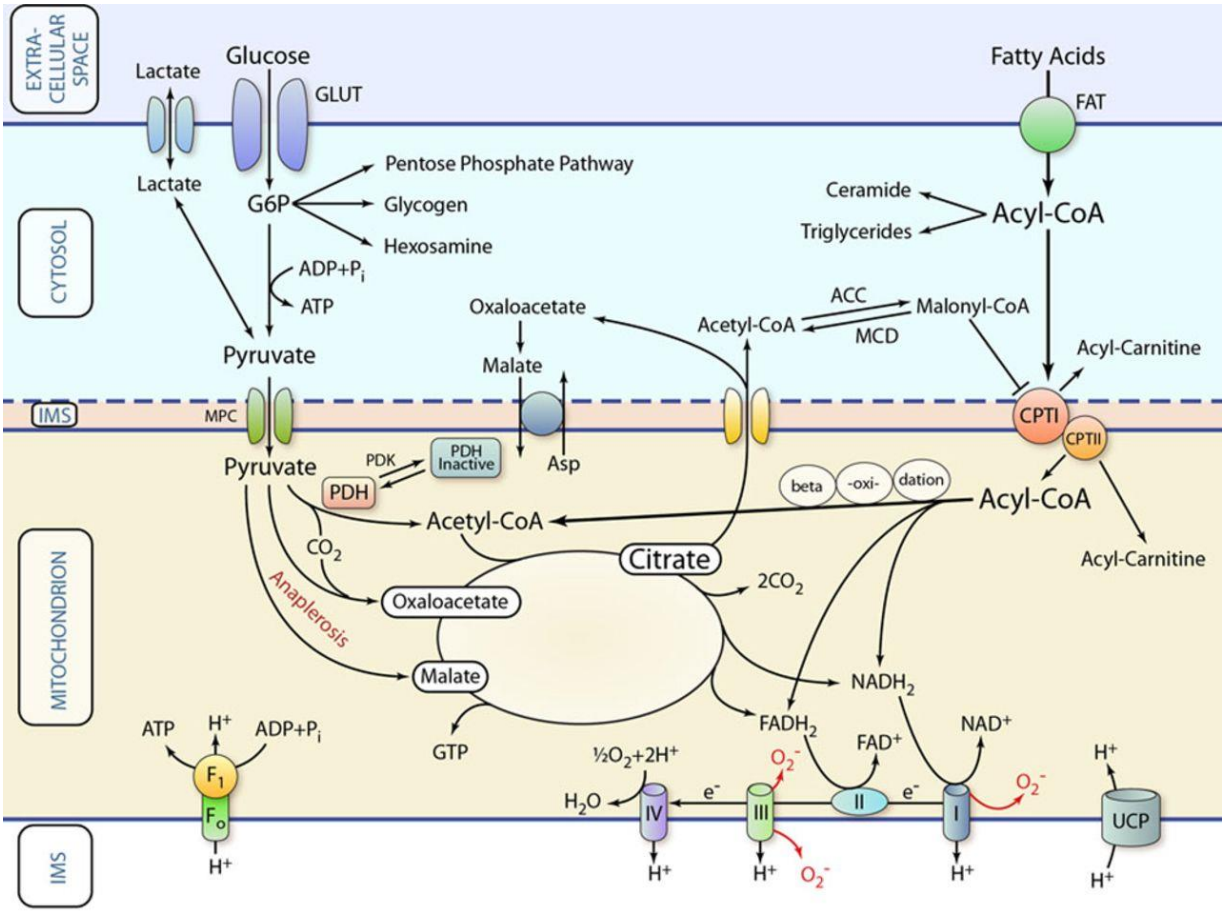

Figure 6. Schematic representation of classic pathways of cardiac metabolism

Even though the heart mainly relies on fatty acid oxidation in order to produce energy, the consumption of excess fats can be potentially detrimental when acetyl-CoA is converted to HMG-CoA. HMG-CoA can then undergo different metabolic processes to form cholesterol. Cholesterol made in excess can block the coronary arteries and cause coronary heart disease (Figure 7).

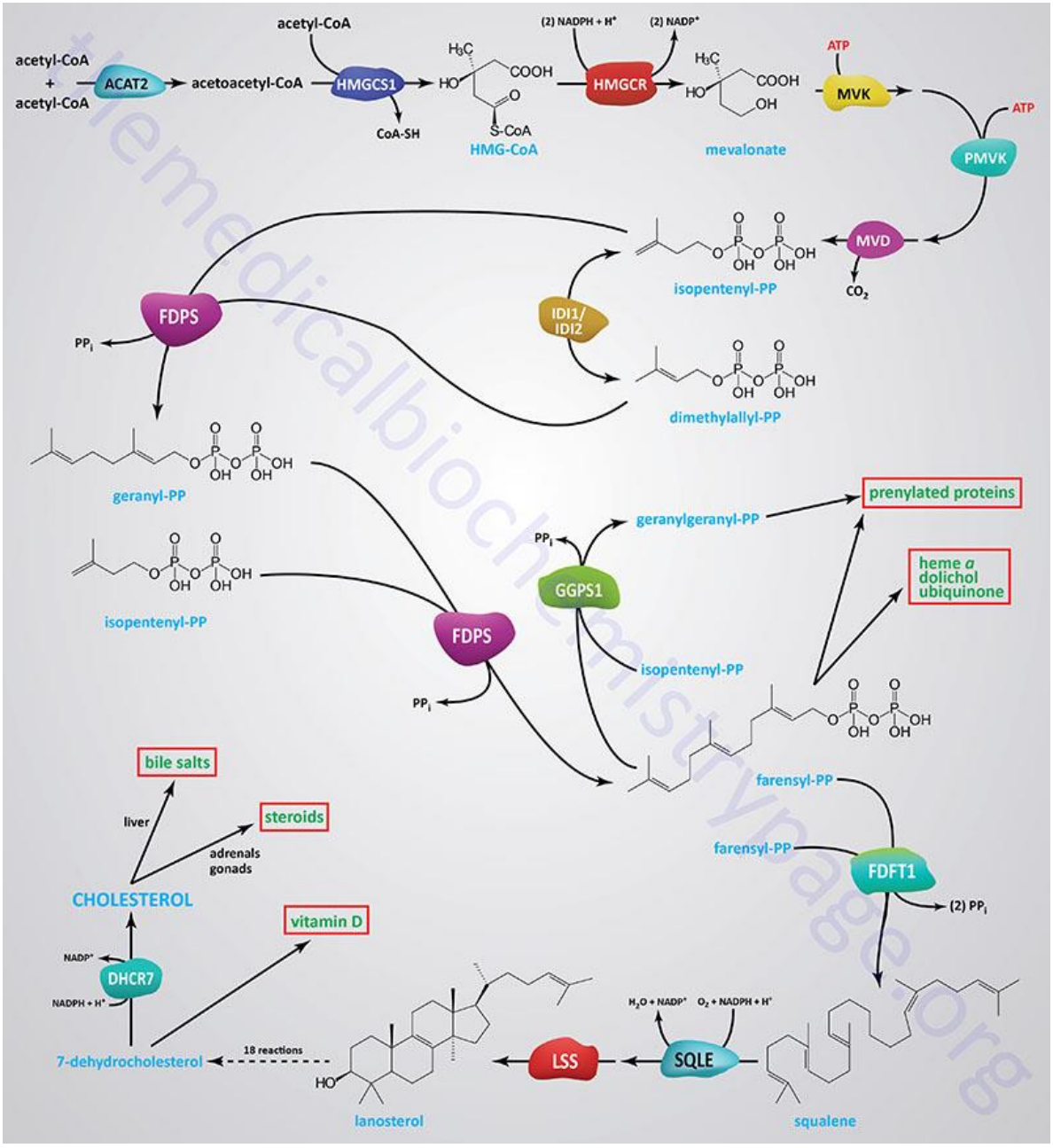

Figure 7. Pathway of cholesterol biosynthesis

1.5 Coronary Heart Disease (CHD)

Heart diseases can be caused by bacteria, viruses, improper opening and closing of the valves, or irregular heartbeat. However, cardiovascular disease specifically deals with conditions where blood vessels are blocked, leading to myocardial infarction/heart attacks, chest pain, and nausea (Mayo Clinic Staff, 2018). This blockage of the blood vessels usually leads to atherosclerosis and ultimately coronary heart disease (CHD).

Atherosclerosis occurs from a buildup of plaque formed by excess cholesterol. The plaque buildup on the vessel walls reduces the diameter of the vessel, thus decreasing the amount of blood to be circulated throughout the heart and, ultimately, the body (AHA Staff, 2017). With diminished blood flow comes diminished oxygen and nutrients circulating in the heart, also accounting for some negative effects of atherosclerosis that leads to CHD.

CHD accounts for 45% of all cardiovascular diseases in the U.S. (AHA, 2016). As with most cardiovascular diseases, the most common sign and symptom of CHD is chest pain (angina). Specifically, the buildup of plaque and stiffening of the coronary arteries causes ischemia, which leads to angina. The ischemia can lead to a myocardial infarction caused by the lack of oxygenated blood reaching certain parts of the heart. During an ischemic period, oxidative phosphorylation will decrease because the cell is forced to switch from aerobic to anaerobic respiration. This switch from aerobic to anaerobic respiration leads to a decrease in the production of ATP, and ultimately, the rate cardiac muscle contraction will decrease as a result of reduced energy (NIH, 2018). Certain risk factors can also contribute to the development of CHD.

1.5.1 Risk Factors of CHD

CHD has multiple risk factors, including age, high blood pressure, and genetics. Just by simply aging, individuals increase their chances of suffering from CHD. Because as one continues to age, the body undergoes the process of senescence where the cell loses the power to divide and grow. Owing to natural "wear and tear" over the years, individuals will not have the ability to repair damaged/blocked vessels the same way their bodies would have had when they were younger, and this inability to repair damaged blood vessels can contribute to arteriosclerosis and eventually CHD.

Another risk factor is uncontrolled high blood pressure/hypertension. Healthy arteries are smooth, strong, and elastic; however, hypertension reduces the characteristics of a healthy artery. Instead of being smooth, hypertension causes the vessels to become rough over an exposed period of high blood pressure, which then leads to the vessel's decreased elasticity/flexibility. Other risk factors include obesity, physical inactivity, and high stress (Mayo Clinic Staff, 2018). The level of intensity or seriousness of each risk factor can have synergistic effects on one another and increase the severity of CHD suffered by an individual. CHD can be divided into acute coronary syndrome and chronic CHD.

Acute coronary syndrome occurs when the coronary arteries suffer from decreased oxygen and blood levels, causing parts of the heart to die (AHA, 2016). Acute coronary syndrome is commonly seen in 3 clinical forms, all related to their appearances in an electrocardiogram (ECG): ST elevation myocardial infarction (STEMI), non-ST elevation myocardial infarction (NSTEMI), and unstable angina. Both STEMI and NSTEMI are types of heart attacks; however, STEMI has full blockage of blood supply causing changes in an ECG

while the opposite is true for NSTEMI (Coronary artery disease types, 2018). Unstable angina, like the name implies, has the individual suffering from varying levels of severity of chest pain. For example, the onset of chest pain could be more frequent or last longer. Note that chronic CHD, also known as stable angina, is the initial manifestation of CHD. Even with individuals suffering from acute or chronic CHD, there are still methods to prevent and treat CHD.

1.5.2 Prevention and Treatment of CHD

Prevention of CHD focuses on individuals following a proper diet, regularly exercising, smoking cessation, and avoidance of trans fats. However, if an individual is already suffering from CHD, different treatment options are available. Treatment for CHD includes medication, such as nitroglycerin or a surgical procedure in the form of angioplasty, stenting, or coronary artery bypass grafting.

Nitroglycerin is used to treat angina because it serves as a vasodilator. It relaxes smooth muscle and blood vessels allowing more blood and oxygen to get to the heart, so the heart does not have to work as hard, thus reducing chest pain (Nitroglycerin, 2018). However, the "gold standard" for treatment of CHD is reperfusion by following angioplastic methods to remove blockages or make repairs in the coronary arteries. Even though reperfusion is the main method for dealing with CHD, it has been shown to provide detrimental effects to the heart as well.

1.6 Reperfusion

Reperfusion is the action of restoring the flow of blood to an organ or tissue typically after a heart attack or stroke. Reperfusion is of the utmost importance because the major complication of CHD is decreased blood flow and oxygen availability. The reintroduction of

proper blood flow eventually alleviates most of the problems caused by the narrowed arteries. However, studies have shown that reperfusion can actually be detrimental to the heart and can further damage the heart after an ischemic episode (Kalogeris, 2014). The additional damage by the reintroduction of blood flow is termed “reperfusion injury.”

Reperfusion injury is exactly as the name implies. The absence of oxygen and nutrients from blood during the ischemic period creates a condition in which the restoration of circulation results in inflammation and oxidative damage through the induction of oxidative stress instead of restoring normal cardiac function (Subodh Verma, 2002).

1.6.1 Pathophysiology of Reperfusion Injury

During ischemia the heart suffers low levels of oxygen. The decrease in oxygen causes the cardiomyocyte to switch from aerobic to anaerobic respiration. This switch causes two main problems: (1) lactate concentration increases and decreases the pH within the cardiomyocyte to acidic levels and (2) oxidative phosphorylation stops. The excess H+ produced by the lactate activates the Na-H exchanger to expel the H+ and bring Na+ into the cardiomyocyte, while at the same time expelling the excess Na+ brought in by the Na-H exchanger using the Na-Ca exchanger which increases the Ca2+ concentration in the cytosol. The decrease in oxidative phosphorylation means that the mitochondria no longer produce ATP needed for normal contraction and relaxation in the heart (Hausenloy & Yellon, 2013) (Figure 8).

During reperfusion, the heart no longer suffers hypoxia and there is an immediate washout of the lactic acid. The quick removal of the lactic acid increases the pH dramatically which leads to series of damaging effects. Mitochondrial re-energization also occurs during reperfusion and allows for the recovery of the mitochondrial membrane potential that drives the

entry of calcium into mitochondria via the mitochondrial calcium uniporter, and ultimately induces mitochondrial permeability transition pore (MPTP) opening (Hausenloy & Yellon, 2013). MPTP is a non-selective channel on the inner mitochondrial membrane. Opening the MPTP causes depolarization and decreases oxidative phosphorylation, leading to decreased ATP production and ultimately death (Hausenloy & Yellon, 2013). The free radicals damage the sarcoplasmic reticulum and cause Ca2+ to leak out. The excess Ca2+ from the damaged sarcoplasmic reticulum and the excess Ca2+ brought in initially by the Na-Ca exchanger during ischemia causes the myofibers to hyper contract (Figure 8).

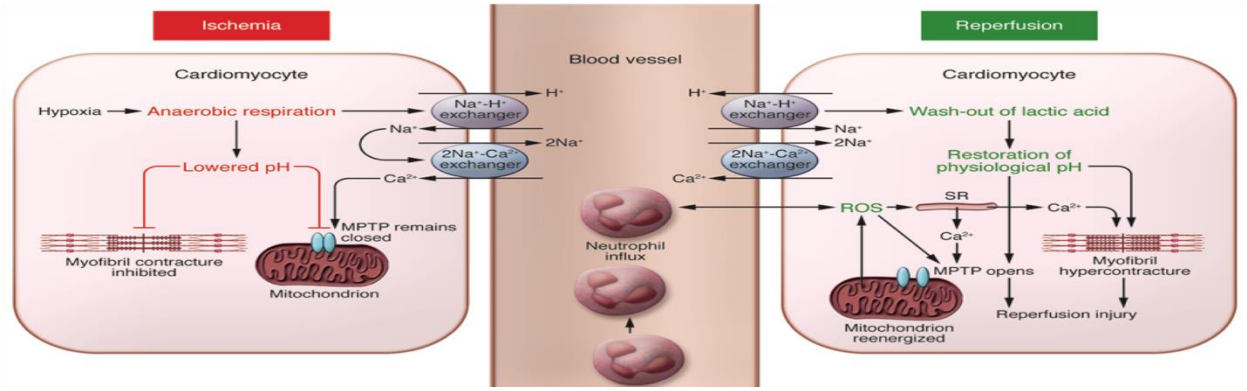

Figure 8. Pathophysiology of Ischemia and Reperfusion Injury

1.6.2 Types of Reperfusion Injury

Reperfusion injury can be categorized into reversible and irreversible reperfusion injury. Reperfusion-induced arrhythmias and myocardial stunning fall under reversible reperfusion injury, while microvascular obstruction and lethal myocardial reperfusion fall under irreversible

reperfusion injury. Reperfusion-induced arrhythmias are irregular heart rates caused by the restoration of blood flow to an area of the heart that was previously exposed to ischemia (Manning & Hearse, 1984). Myocardial stunning is a post-ischemic dysfunction resulting from oxidative stress and intracellular calcium overload on the heart's contractile abilities and is the best-known form of reperfusion injury (Subodh Verma, 2002) (Hausenloy & Yellon, 2013).

Microvascular obstruction is defined as the inability to reperfuse a previously ischemic area caused by capillary compression from plaque accumulation, cardiomyocyte swelling, and neutrophil plugging (Hausenloy & Yellon, 2013). Activated endothelial cells within the blood vessels produce more reactive oxygen species (ROS) but less nitric oxide (NO) following reperfusion.

Lethal myocardial reperfusion injury is caused by oxidative stress or calcium overload. Oxidative stress occurs rapidly during myocardial reperfusion and as such researchers decided that an antioxidant during this period of reperfusion would help reduce injury; however, the beneficial results of the experimental and clinical studies were mixed and uncertain (Hausenloy & Yellon, 2013). Intracellular and mitochondrial calcium overload begins during ischemia and progressively gets worse during reperfusion because of damage to the sarcoplasmic reticulum and mitochondrial re-energization.

Cardiac tissue and muscle are like neurons in that once a portion of cardiac tissue or muscle dies it cannot be regenerated and is lost forever. However, there is another method researchers are looking into that may be able to decrease infarct size in cardiomyocytes that may have suffered from reperfusion injury or a heart attack. In particular, researchers believe that targeted modulation of autophagy in heart cells may render cardiomyocytes resistant to ischemia

or reperfusion injury and have longer term positive protective effect on cardiac function (Przyklenk, Dong, Undyala, & Whittaker, 2012).

1.7 Autophagy

Autophagy is the controlled digestion of damaged organelles within a cell. It is tightly regulated intracellular catabolic system that delivers degraded cytoplasmic constituents to the lysosome. It consists of several sequential steps: sequestration, transportation to the lysosome, degradation, and utilization of the degraded products (Mizushima, 2007). The goals of the process are to reduce the number of damaged organelles or protein aggregates in compromised cells and to save and recycle amino acids and other substrates needed for protein synthesis and ATP generation (Mizushima, 2007). So far, approximately 30 autophagy-related genes (Atg) have been discovered.

During autophagy induction, contents from the cytoplasm are sequestered by an isolation membrane, and complete sequestration forms a double-membraned organelle (i.e., autophagosome). The compositions of the inner and outer membranes are different in that the inner membrane has the microtubule associated protein 1 light chain 3 (LC3-1), which is converted to LC3-2 when linked to phosphatidylethanolamine (Belzile et al., 2016). Therefore, LC3-1 is found on the outer membrane and LC3-2 is found on the inner membrane of the autophagosome. LC3-2 functions as a nonpolar receptor for p62, which works in multiple signaling pathways for apoptosis, and also serves as a marker of autophagy induction (Mizushima, 2007).

The apoptotic marker p62, also known as the sequestosome (SQSTM1), is found in polyubiquinated protein aggregates and binds directly to LC3-2 (Serhiy Pankiv et al., 2007). Once bound, p62 serves as a "signal" to attract damaged proteins and organelles to the autophagosome for degradation.

For degradation to occur, the autophagosome fuses with the lysosome to form the autolysosome, and the contents within the autolysosome are destroyed by lysosomal hydrolases. After the macromolecules have been degraded, the micro molecules are taken to the cytoplasm to be recycled (Mizushima, 2007). The recycled amino acids provide the metabolic precursors for cardiac development and provides a method of cardiac protection (Yan, 2009).

1.7.1 Regulation of Autophagy

The most common trigger of autophagy is starvation or a lack of nutrients in the body. In mammals, autophagy occurs when there is a lack of amino acids ((Mizushima, 2007). Under these conditions, Beclin-1 and Class 3 phosphatidylinositol kinase (PI3K) levels in the cell are increased. Beclin-1 is an autophagy-associated tumor suppressor and is distributed within the plasma membrane, cytoplasm, and nucleus (Kang, Zeh, & Tang, 2011). Beclin-1 has several structural domains, but the most important is the evolutionarily conserved domain which is essential for promoting Beclin-1's autophagy-inducing properties and for inhibiting tumorigenesis (Kang et al., 2011).

Phosphatidylinositol kinase regulates a variety of signaling, trafficking, and metabolic processes. Specifically, Class 3 PI3K (also known as Vps34) deals with membrane trafficking by promoting endosomal protein sorting, endosome-lysosome maturation, and ultimately

autophagosome formation (Jean, Steve and Kiger, Amy, 2014). Also, Class 1 PI3K inhibits autophagy via phosphorylation of Akt (i.e., a signal transducer that promotes survival and growth) and activation of the mammalian target of rapamycin (mTOR), a signal for nutrient availability.

A general pathway for autophagy induction is as follows: a stress signaling kinase (e.g. JNK-1) phosphorylates Bcl-2. The phosphorylation of Bcl-2 allows Beclin-1 to dissociate from Bcl-2 and interact with Class 3 PI3K. The interaction between Beclin-1 and Class 3 PI3K promotes the conjugation of different Atg, and the Atg conjugation supports the conversion of LC3-1 to LC3-2. Once damaged proteins enter the isolation membrane, the membrane elongates until it closes to become the autophagosome. The autophagosome fuses with the lysosome to form the autolysosome, where the damaged proteins or organelles are broken down and used as precursors for other metabolic activity (Figure 9).

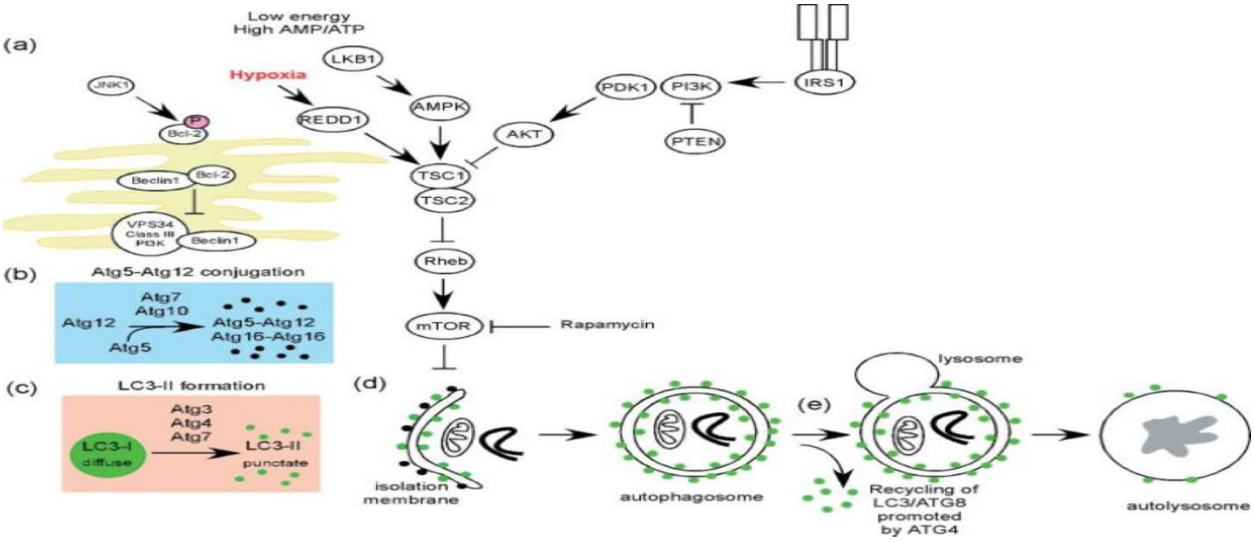

Figure 9. Signaling pathway for autophagy

1.7.2 Mammalian Target of Rapamycin (mTOR)

A key regulator of autophagy in mammalian cells is the kinase mTOR which receives signals from various metabolic processes and growth factors. During growth, the activity of two mTOR complexes (mTORC) is increased by factors that activate Class 1 PI3K pathway, thereby increasing Rheb, a GTPase needed for mTOR activity (Carol Chen-Scarabelli, 2015) (Figure 10). Class 1 PI3K reduces the Atg conjugation, specifically Atg1-Atg13, thus decreasing autophagy induction. The 2 mTOR complexes are mTORC1 and mTORC2. mTORC1 is involved in protein synthesis, energy metabolism, and is inhibited by rapamycin, while mTORC2 regulates the cytoskeleton and is insensitive to rapamycin. See figure 8. However, an mTOR-dependent pathway is not the only autophagy promoter.

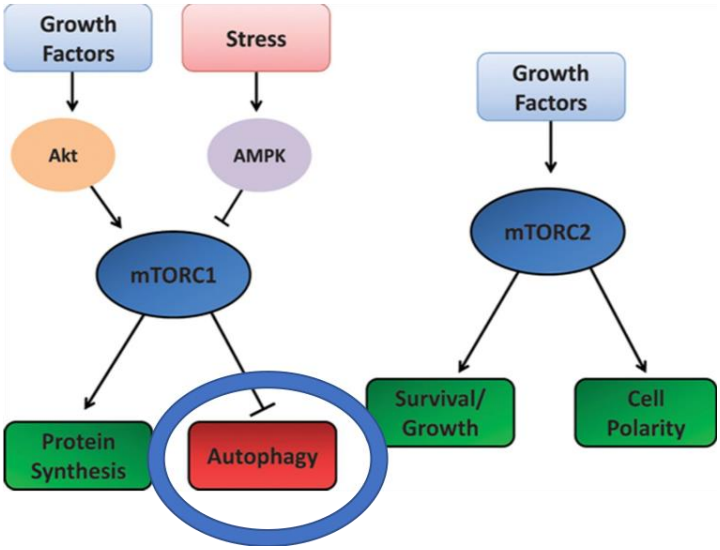

Figure 10. Activation and regulation of mTORC1 and mTORC2

1.7.3 Adenosine Monophosphate-Activated Protein Kinase (AMPK)

Autophagy also can be regulated by AMPK, an AMP/ATP sensor found in mammalian cells. When ATP is depleted, AMP levels rise and "mimic" cell starvation. Low AMP levels lead to AMPK activation, which stimulates energy-generating processes (e.g., fatty acid oxidation) and inhibits energy-consuming processes (e.g. macromolecule synthesis). Activated AMPK can inhibit mTOR by interfering with the GTPase activity of Rheb and with protein synthesis can degrade the phosphorylation of ULK1, the mammalian homologue of Atg1, and promote its destruction from the mTOR compounds and allows for autophagy induction (Richter & Ruderman, 2009).

1.8 Autophagy During Ischemia

In the body, autophagy occurs normally at low basal levels to maintain cell homeostasis by clearing out excess proteins and old organelles. It is upregulated by stress conditions, such as an increase in reactive oxygen species or energy deprivation (Ma, 2014). During ischemia, autophagy is activated by AMPK while mTOR is inactivated (Ma, 2014). In ischemia, the heart is deprived of nutrients and the levels of ATP are decreased. AMPK senses the energy drop caused by an increased ratio of AMP to ATP and begins adapting to the problem of low energy (Figure 11).

Scientists were able to confirm the increased ratio of AMP to ATP by suppressing endogenous AMPK during ischemia and found that myocardial infarct size was increased. However, this study did not directly address the inhibition of autophagy and how it leads to increased infarct size (Qi, 2015) .

To directly address the inhibition of autophagy via decreased AMPK activity, another study explained that without AMPK, ULK1 could not be phosphorylated to promote autophagosome production and ultimately autophagy induction could not occur (Ma, 2014).

1.9 Autophagy During Reperfusion

During reperfusion, the heart is no longer deprived of energy (i.e. decreased ATP), thus, AMPK is inactivated. However, reactive oxygen species produced by damaged mitochondria induce autophagy by activating Beclin-1 and Class 3 PI3K (Zhang, 2013) (Ma, 2014). The increased reactive oxygen species level overstimulates Beclin-1, leading to autophagic cell death by the destruction of both damaged and undamaged cells (Zhang, 2013). Therefore, autophagy during reperfusion can either be beneficial or detrimental, depending on the length and intensity of autophagy (Figure 11).

Reactive oxygen species also contributes to autophagy induction during reperfusion by inhibiting the activity of Atg4, leading to protein lipidation, causing improper protein-protein attachments, and ultimately protein aggregation.

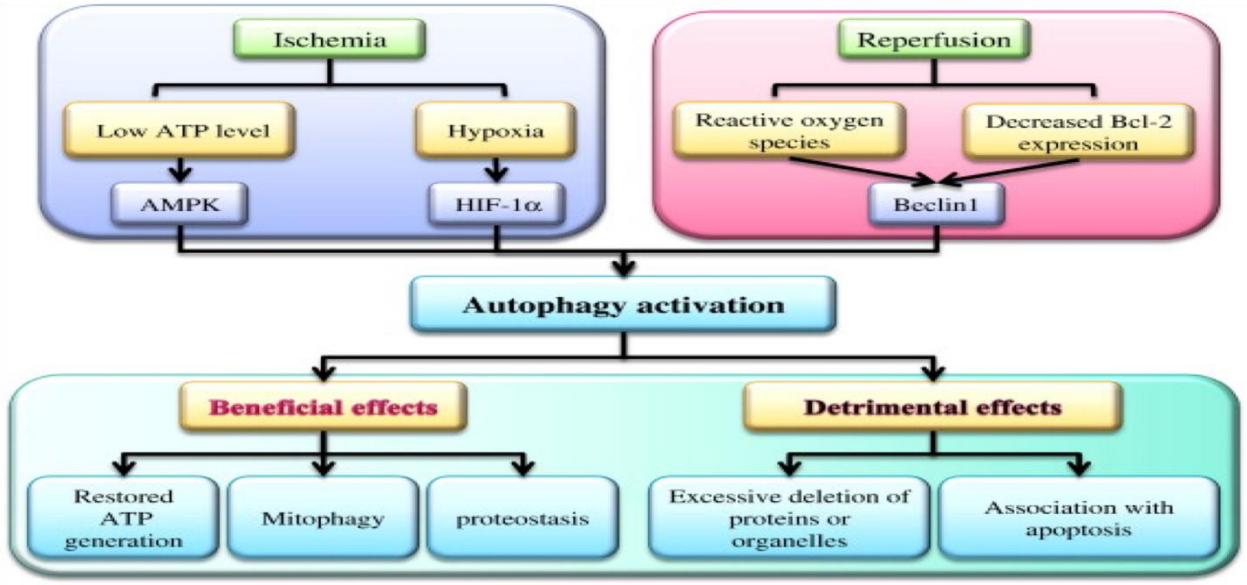

Figure 11. Autophagy activation

1.10 Autophagy in Pre-conditioning Models

In pre-conditioning models, cycles of transient ischemia/reperfusion are employed to induce autophagy. Another method is to induce autophagy directly with an autophagy drug enhancer. A study using swine models reported a 60% decrease in infarct size for pre-conditioned models when autophagy was enhanced (Yan, 2009). Pre-conditioning increases the expression of the autophagy-related proteins LC3-2 and Beclin-1 and promotes autophagosome formation (Zhang, 2013). However, excessive autophagy can also cause cell death directly by degrading too many organelles or indirectly by communicating with apoptotic pathways. The lysosomes that degrade autophagic sequestration are not involved in necrosis but are involved in apoptosis. This occurs because autophagy activation leads to increased levels of lysosomal hydrolases that are involved in caspase activation and the subsequent apoptosis process (Zhang, 2013).

1.11 Autophagy in Post-Conditioning Models

In post-conditioning models, an autophagy enhancing drug is given at the beginning of reperfusion and infarct size is recorded afterwards. A study conducted with isolated rat hearts used ischemic post-conditioning as a means of cardio protection against ischemia/reperfusion injury. The results suggest researchers found that enhanced autophagy induction during post-conditioning allows for cardio protection by decreasing calcium overload, reducing oxidative stress, and inhibiting necrosis & apoptosis (Rui Sheng & Zheng-hong Qin, 2015). This study also found an increase in the autophagic-related proteins LC3-2 and Beclin-1. However, other studies have omitted using autophagy in post-conditioning models and rely solely on pre-conditioning models because of the reported detrimental effects that occur during reperfusion when autophagy is enhanced.

1.12 Autophagic Drug Enhancers & Inhibitors

1.12.1 Rapamycin

Rapamycin, also known as Sirolimus, is a macrocyclic antibiotic made by the bacterium Streptomyces hygroscopicus that inhibits the proteins serine, threonine, and Class 1 PI3K of mTOR (Ballou & Lin, 2008). Rapamycin forms a gain-of-function complex w/an FKBP12 protein, and this complex binds and specifically acts as an allosteric inhibitor of mTOR (Ballou & Lin, 2008) (Figure 12).

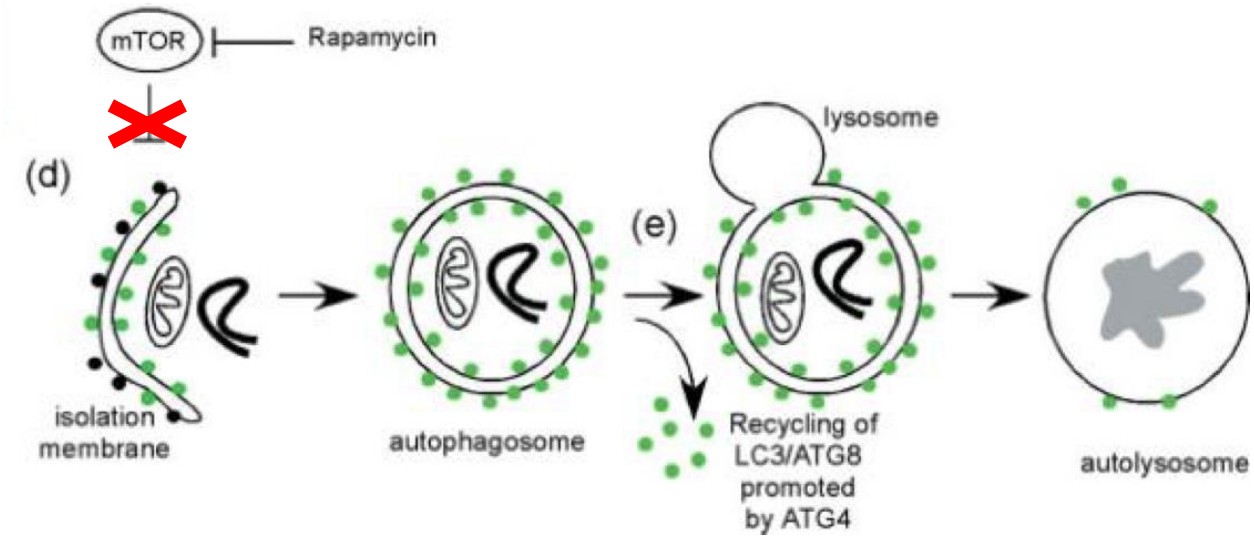

Figure 12. How rapamycin blocks mTOR and induces autophagy

1.12.2 Trehalose

Trehalose is a non-toxic disaccharide found in plants and insects, but not in mammals. In organisms with trehalose, it serves as a protein chaperone and stabilizes the cell membrane (Mardones, Rubinsztein, & Hetz, 2016). Trehalose is able to activate autophagy by inhibiting various glucose transporters at the plasma membrane, causing AMPK to be activated and phosphorylation of the kinase ULK-1. It has also been noted that because of trehalose protein chaperone ability, that it is able to work independent of the mTOR (Mardones et al., 2016) (Figure 13).

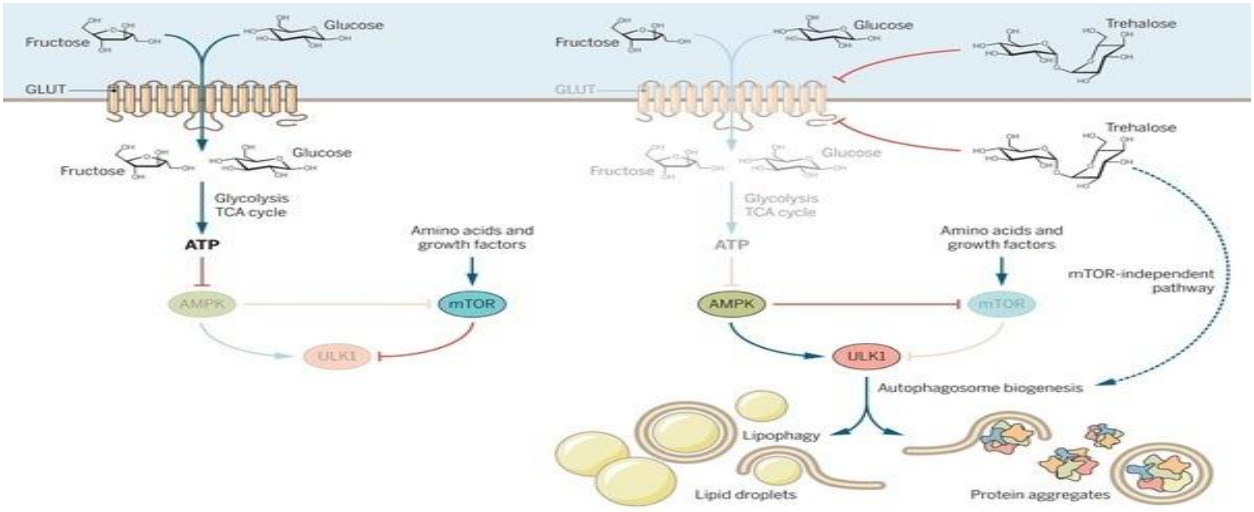

Figure 13. How trehalose induces autophagy

1.12.3 3-Methyladenine (3-MA)

3-MA is used to inhibit autophagy under various conditions, by blocking autophagosome formation via inhibition of Class 3 PI3K, which is essential for recruitment and elongation of the isolation membrane for autophagy induction (Sigma-Aldrich, 2017) (Figure 14).

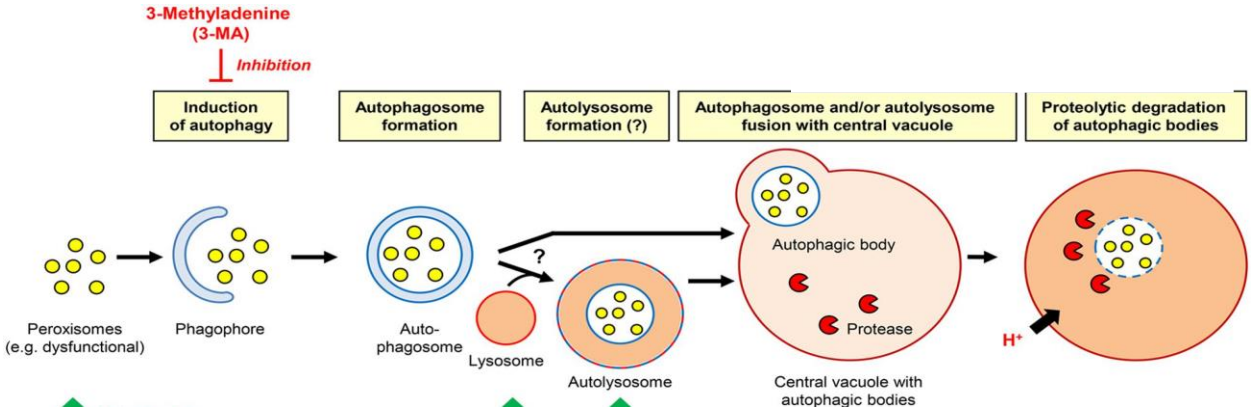

Figure 14. How 3-MA inhibits autophagy induction

METHODS

2.1 Animals

All animal procedures were approved by the Institutional Animal Care and Use Committee at PCOM for care and use of animals. Male Sprague Dawley (SD) rats (275-325g; Ace Animals, Boyertown, PA) were used in our study.

2.2 Krebs Buffer Solution

This buffer solution will provide the isolated heart with necessary molecules and nutrients for normal contraction and prevent arrhythmias. The krebs buffer is placed in warm water where it is allowed to reach and maintain a constant temperature of 37 degrees Celsius similar to that internal body temperature of SD rats.

In addition, the krebs buffer was maintained at a constant pressure of 80mmHg. It was important to aerate the buffer with 95% O2 : 5% CO2 in order to prevent crystallization of calcium, which would impede the flow of buffer to the isolated SD rat heart, and maintain the buffer pH at 7.3 to 7.4 and also assists in the production of ATP.

2.3 Isolated Rat Heart Preparation

SD rats were first anesthetized with pentobarbital sodium 60mg/kg and injected with 1mL of sodium heparin (1000U) intraperitoneally to prevent blood coagulation; afterwards the heart was rapidly excised and placed in ice cold buffer.

The Langendorff Perfused Heart Technique was used for the heart perfusion (Doring, 1990). Following this technique, the isolated SD rat heart was cannulated via the aorta onto a perfusion needle and immersed into 160mL of warm krebs buffer. The hearts were continuously

perfused with krebs buffer (37 degrees Celsius and approximately 7.4pH) before global ischemia and during reperfusion.

A side arm in the perfusion line proximal to the heart inflow cannula allowed infusion of either buffer (for sham group) or the drug of choice at a rate of 1mL/min (Figure 15).

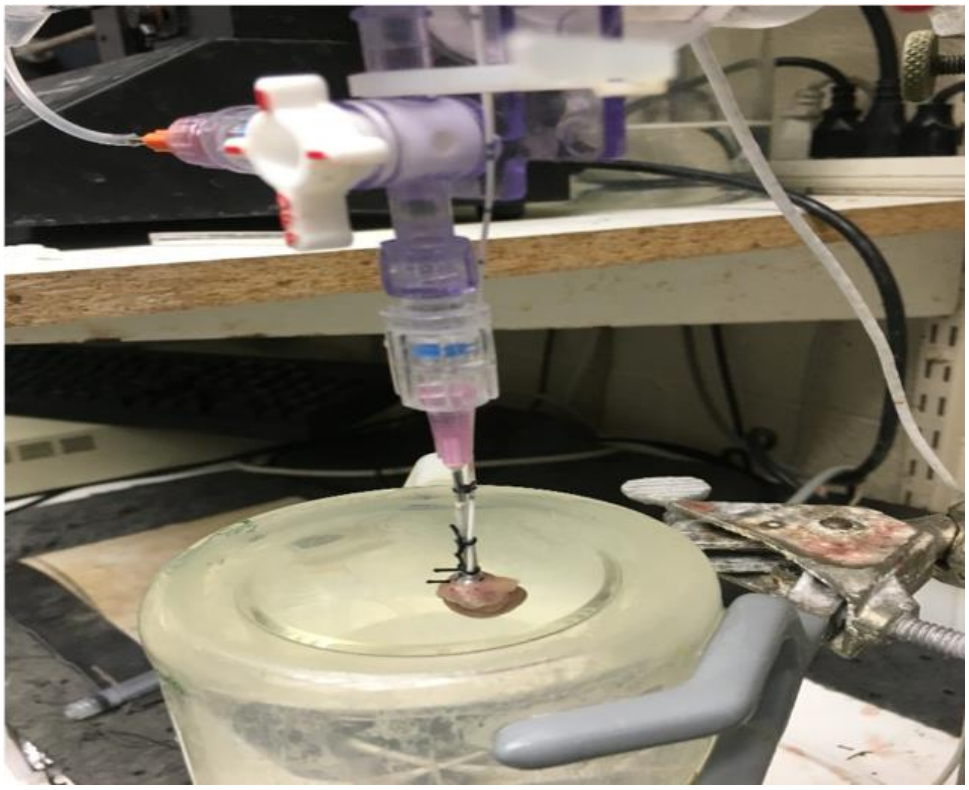

Figure 15. Langendorff preparation with isolated heart cannulated to perfusion needle

2.3.1 Cardiac Parameters

Coronary flow (CF), measured in mL/min, was recorded by a flowmeter (T106, Transonic Systems, Inc., Ithaca, NY). A pressure transducer was placed into the left ventricle of the isolated SD rat heart and allowed for the measurement of several cardiac functions including: left ventricular end systolic pressure (LVESP), left ventricular end diastolic pressure (LVEDP),

left ventricular developed pressure (LVDP). The maximum and minimal rate of pressure change (i.e. derivative pressure/derivative time= +dP/dt Max and -dP/dT Min, respectively) as well as the heart rate, were monitored using the pressure transducer (SPR-524, Millar Instruments, Inc., Houston,TX) and recorded using a Powerlab Station acquisition system (AD Instruments, Grand Junction, CO).

2.3.2 Staining to Evaluate Infarct Size

The isolated heart was removed from the perfusion apparatus at the end of the experimental procedure and placed in a freezer for approximately 20 minutes, then cut into cross sectional slices from the base to the apex, which were placed in a 1% solution of 2,3,5-triphenyltetrazolium chloride (TTC) for 5 to 7 minutes. TTC is a colorless water-soluble dye that is taken up by the mitochondria of living cells and then reduced to a deep red, water-insoluble formazan compound (Sigma Aldrich, 2018). The enzyme dehydrogenase converts the TTC to its red color. In non-viable cells dehydrogenase is no longer found and is unable to promote TTC change to its red color, thus leaving the dead cells white.

The purpose of staining is to expose the areas where the myocardium is necrotic. Pictures of the infarct areas were compared between control and drug-treated hearts. After staining is complete the heart slices are placed in formaldehyde to be fixed. The whole heart is first weighed out then pale/white areas (i.e. dead areas due to I/R injury) are cut and separately weighed, giving the dead heart weight. Afterwards, both the total and dead heart are placed in 4% formaldehyde, labeled, and refrigerated (Figure 16). Infarct size (%) = (dead heart/total heart) x 100

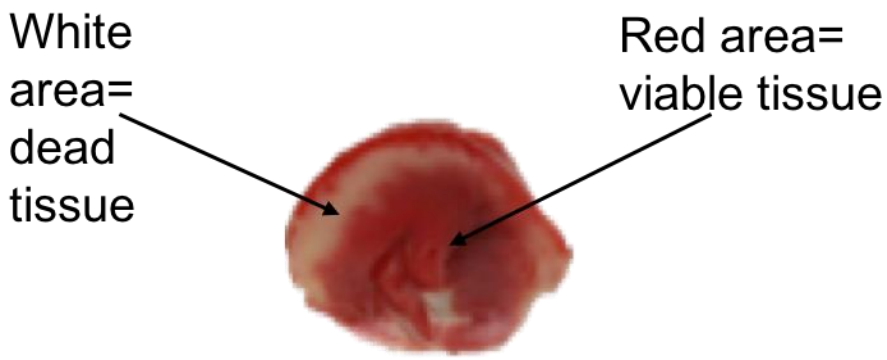

Figure 16. Infarction of isolated SD heart

2.4 Study Groups

Multiple groups were studied to test whether autophagy enhancement was beneficial and/or detrimental to cardiac function (Figure 17).

Figure 17. Flow diagram of experimental protocol

2.4.1 Sham Control

The isolated heart was perfused with normal Krebs' buffer for the experimental periods, including baseline (20 min), pseudo-ischemia (30 min), and pseudo-reperfusion (45 min) without induction of ischemia to determine if cardiac function can be maintained in this Langendorff preparation for the length of experimental procedure without any tissue damage by evaluating for the presence of infarction.

2.4.2 Ischemia/Reperfusion (I/R) Control

After baseline recording of cardiac function and coronary flow, the isolated heart ischemia was induced by stopping perfusion of normal Krebs' buffer for 30 minutes, then restart perfusion of normal Krebs' buffer (R) for 45 minutes. Infarct size was determined at the end of experiments. The isolated heart was only infused with Krebs' buffer either before ischemia or at the beginning of reperfusion to determine the in cardiac function and infarct size after an I/R insult.

2.5 Rapamycin Pre-treatment with I/R Group

After baseline recording of cardiac function and coronary flow, 25nM rapamycin was dissolved in Krebs' buffer and infused for 5 min just before initiation of ischemia to determine if rapamycin pre-treatment would restore post-reperfused cardiac function and reduce infarct size.

2.5.1 Rapamycin Post-treatment with I/R Group

After baseline recording of cardiac function and coronary flow, 25nM rapamycin was dissolved in Krebs' buffer and infused for 5 minutes at the beginning of reperfusion and not before an ischemic episode. Post-reperfused cardiac function and infarct size were measured at the end of the experiment.

2.6 Trehalose Pre-treatment with I/R group

After baseline recording of cardiac function and coronary flow, 5mM trehalose was dissolved in Krebs' buffer and infused for 5 minutes before initiation of ischemia to determine if trehalose pre-treatment would restore post-reperfused cardiac function and reduce infarct size.

2.6.1 Trehalose Post-treatment with I/R Group

After baseline recording of cardiac function and coronary flow, 5mM trehalose was dissolved in Krebs' buffer and infused for 5 minutes at the beginning of reperfusion and not

before an ischemic episode to determine if post-reperfused cardiac function was restored and infarct size reduced.

2.7 3-Methyadenine (3-MA) Pretreatment with I/R Group

After baseline recording of cardiac function and coronary flow, 1mM 3-MA was dissolved in Krebs' buffer and infused for 5 minutes before initiation of ischemia to determine if 3-MA pre-treatment would further impair post-reperfused cardiac function and increase infarct size.

2.7.1 3-Methyadenine Posttreatment with I/R Group

After baseline recording of cardiac function and coronary flow, 1mM 3-MA was dissolved in Krebs' buffer and infused for 5 minutes at the beginning of reperfusion and not before an ischemic episode to determine if post-reperfused cardiac function was further compromised and infarct size increased.

2.8 Drug Preparation

2.8.1 Drug PRE-treatment Preparation

Rapamycin (stock solution= 5mM): 25nM[rapamycin] infused for 5 minutes at 1mL per minute. To calculate how much rapamycin should be taken out of the stock solution: [rapamycin nM] x coronary flow x (minutes of reperfusion + 2mL of tube dead space).

Stock solution: E.g. (25nM rapamycin) x (17mL/min) x (5 minutes of reperfusion + 2mL of tube dead space). 5mM stock solution rapamycin = 0.51uL of rapamycin to be taken from rapamycin stock solution and added to 7mL of Krebs Buffer Solution for infusion before ischemic episode

Trehalose: 5mM [trehalose] infused for 5 minutes at 1mL per minute. To calculate how much trehalose should be taken out of the stock solution: [trehalose] x coronary flow x (minutes

of reperfusion + 2mL of tube dead space) x trehalose molecular weight. E.g. 5mM trehalose x 13mL/min x 7mL x 0.37833g/mol trehalose= 172mg of trehalose to be obtained from stock bottle and added to 7mL of Krebs Buffer Solution for infusion before ischemic episode.

*3-Methyladenine (3-MA):*1mM [3-MA] infused for 5 minutes at 1mL per minute. To calculate how much 3-MA should be taken out of stock solution: [3-MA] x coronary flow x (minutes of reperfusion + 2mL of tube dead space) x 3-MA molecular weight. E.g. (1mM 3-MA) x (20mL/min) x (5 minutes of reperfusion + 2mL of tube dead space) x 149.2g/mol 3-MA=0.0208g of 3-MA to be obtained from stock bottle and added to 7mL of Krebs Buffer Solution for infusion before ischemic episode.

2.8.2 Drug POST-treatment Preparation

Note that for all post-treatment groups drug calculation is based on a coronary flow of 10mL/min. Rapamycin (same method as pretreatment, but given immediately after ischemic episode/beginning of reperfusion). Trehalose (same method as pretreatment, but given immediately after ischemic episode/beginning of reperfusion).3-MA (same method as pretreatment, but given immediately after ischemic episode/beginning of reperfusion).

2.9 Statistical Analysis

All data in the following text and figures are presented as means ± standard error. The data was analyzed by variance, using post hoc analysis with the Student-Newman-Keuls test. Probability values of $p<0.05$ are considered statistically significant.

RESULTS

3.1 Left Ventricular End Diastolic Pressure (LVEDP)

Initial LVEDP among all groups were similar. The control I/R group showed a very high final LVEDP level. By contrast, autophagy enhancement as pre or post-treatment, in both rapamycin and trehalose treated groups, showed a decrease in final LVEDP compared to that of control I/R. Rapamycin pre-treatment showed the lowest final LVEDP ($p<0.05$). However, autophagy inhibition as pre or post-treatment with 3-MA did not show any significant change in final LVEDP when compared to control I/R group (Figure 18a).

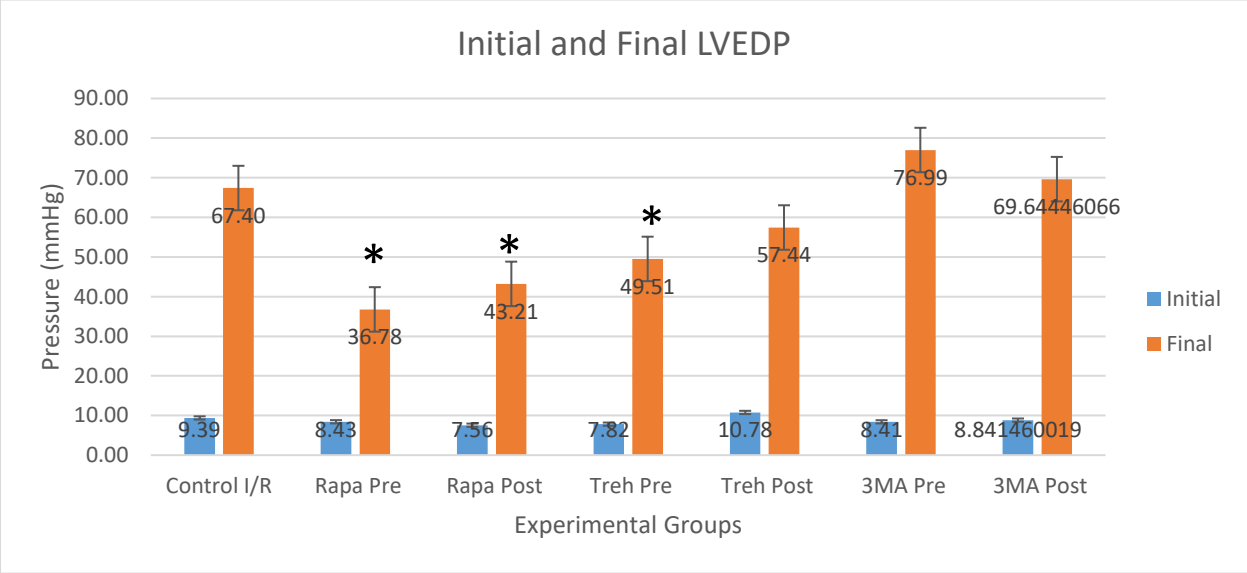

Figure 18a. Initial and final LVEDP values of control I/R, autophagy enhancement groups, and autophagy inhibitor groups. Asterisks (*) was used to represent significance compared to final control I/R group.

Time course of LVEDP for control I/R and both rapamycin treatment groups are illustrated in Figure 18b. The control I/R group showed a dramatic increase in LVEDP at 5 minutes (75.5 ±

14.9 mmHg) compared to its initial value (9.4 ± 3.1 mmHg). Then the LVEDP level remained relatively constant throughout the reperfusion time but never returned to its initial value. At the end of reperfusion, the LVEDP was 36.8 ± 16.7. Moreover, both rapamycin treatments had initially increased LVEDP levels but reduced afterwards. However, rapamycin pre-treatment significantly improved LVEDP starting from 15 minutes and continued to the end of reperfusion when compared to control I/R (all $p<0.05$). Rapamycin post-treatment showed significant improvement of LVEDP from 35 to 45 minutes reperfusion (all $p<0.05$). By contrast, rapamycin pre-treatment showed more improved LVEDP values throughout reperfusion when compared to rapamycin post-treatment, however, these LVEDP values were not significant.

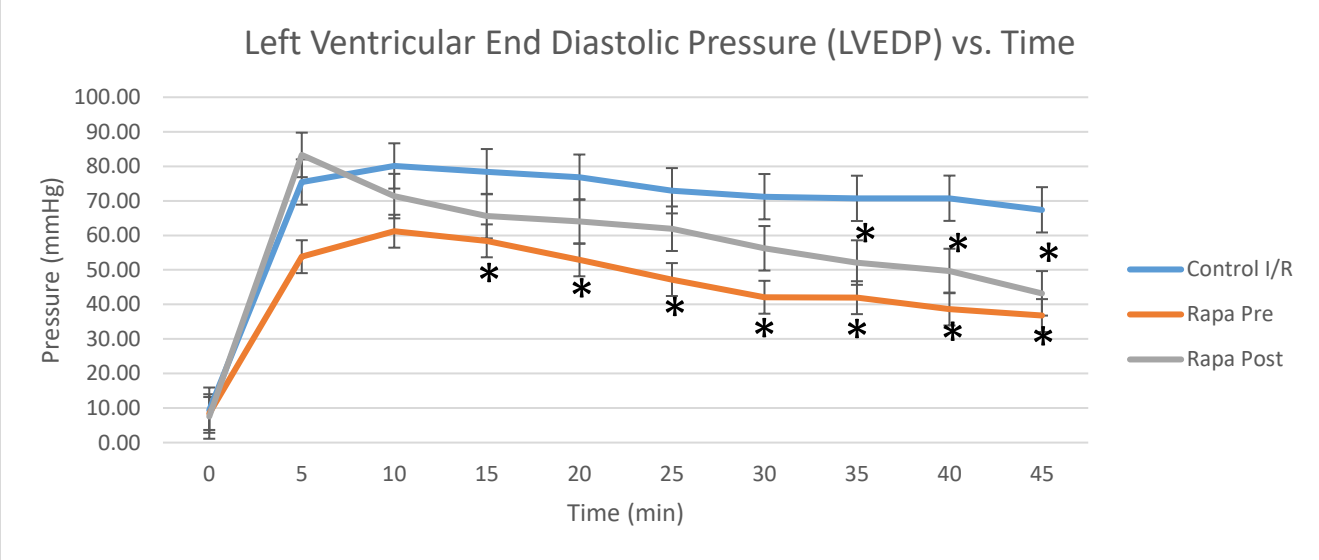

Figure 18b. Time course of rapamycin LVEDP. Asterisk (*) indicates significant difference between either rapamycin treatment groups when compared to control I/R.

Time course of LVEDP for control I/R and both trehalose treatment groups are illustrated in Figure 15c. Compared to the control I/R group, trehalose pre and post-treatment followed a similar trend of initially having compromised LVEDP values at 5 minutes (69.3 ± 22.7 mmHg

and 62.3 ± 23.4 mmHg, respectively) compared to their initial values (7.8 ± 3.1 mmHg and 10.8 ± 6.0 mmHg, respectively), and remained constant throughout the reperfusion period. Trehalose pre-treatment showed significantly improved LVEDP at 10, 20, 25, 30, 35, and 45 minutes reperfusion, while trehalose post-treatment only showed significantly improved LVEDP at 30 minutes reperfusion ($p<0.05$). Trehalose pre-treatment showed more improved LVEDP values starting from 15 to 45 minutes reperfusion when compared to trehalose post-treatment, however, the values were not significant. Autophagy inhibitor group time points were not included because there was no significance of LVEDP when compared to control I/R group at any time point.

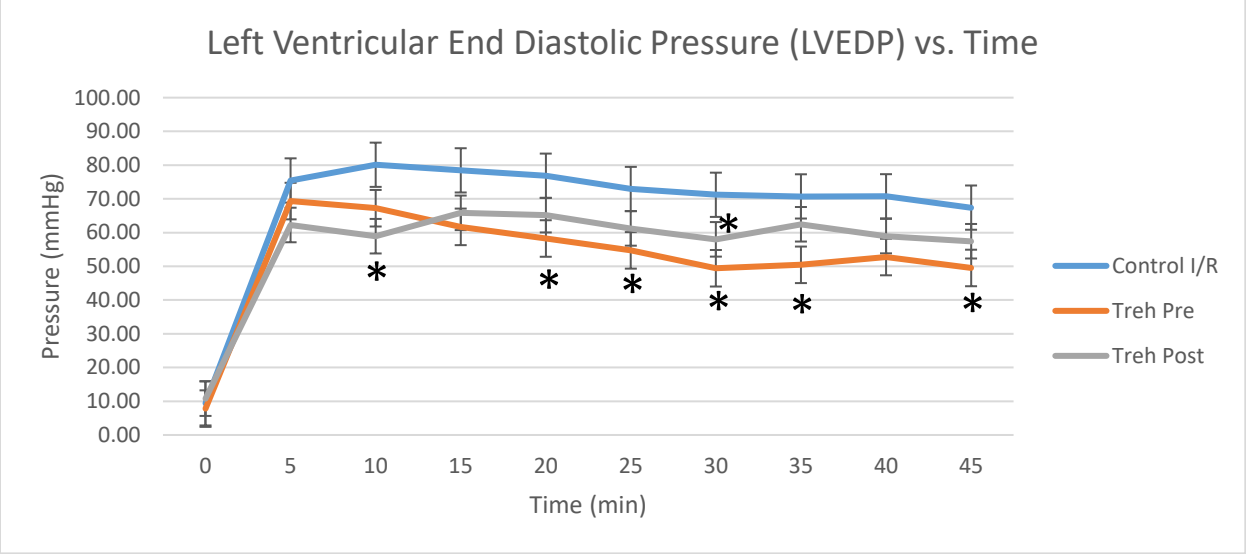

Figure 18c. Time course of trehalose LVEDP. Asterisk (*) indicates significant difference between either trehalose treatment groups when compared to control I/R.

3.2 Left Ventricular End Systolic Pressure (LVESP)

Initial LVESP among all groups were similar. Compared to final LVESP in control I/R group, autophagy enhancers and inhibitor did not show a significant difference when comparing

initial and final LVESP levels. The time course for LVESP was not provided because no significance occurred between any of the groups at any time points (Figure 19).

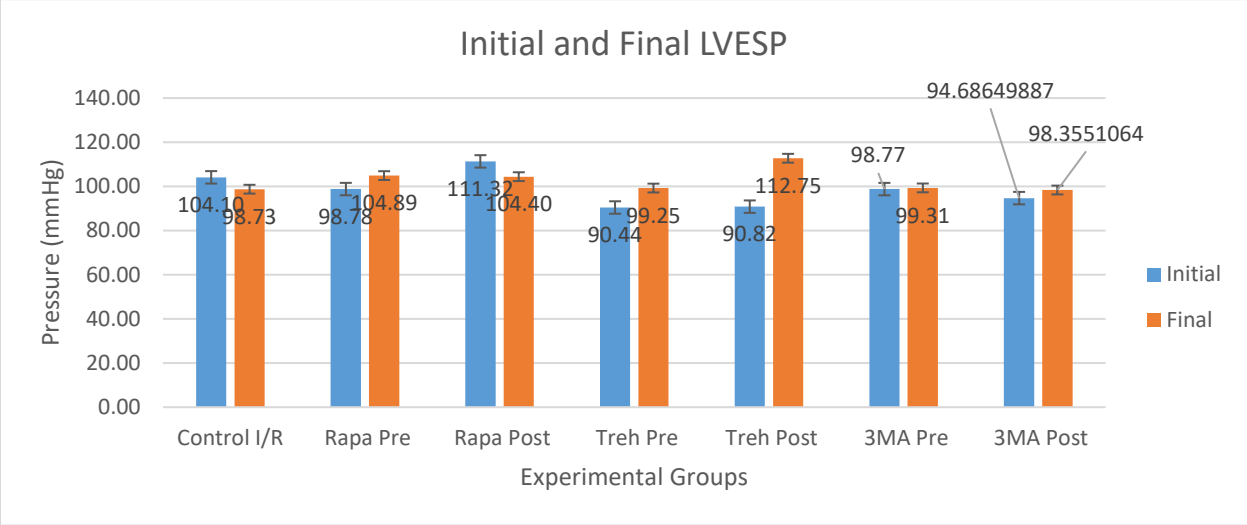

Figure 19. Initial and final LVESP values of control I/R, autophagy enhancement groups, and autophagy inhibitor groups

3.3 Left Ventricular Developed Pressure (LVDP)

Initial LVDP among all groups were similar and the control I/R showed a decrease in final LVDP. By contrast, autophagy enhancement as pre or post-treatment with rapamycin or trehalose showed an improvement in final LVDP when compared to final control I/R ($p<0.05$). Rapamycin pre-treatment had the highest final LVDP value. However, autophagy inhibition as pre or post-treatment did not improve final LVDP when compared to control I/R. (Figure 20a).

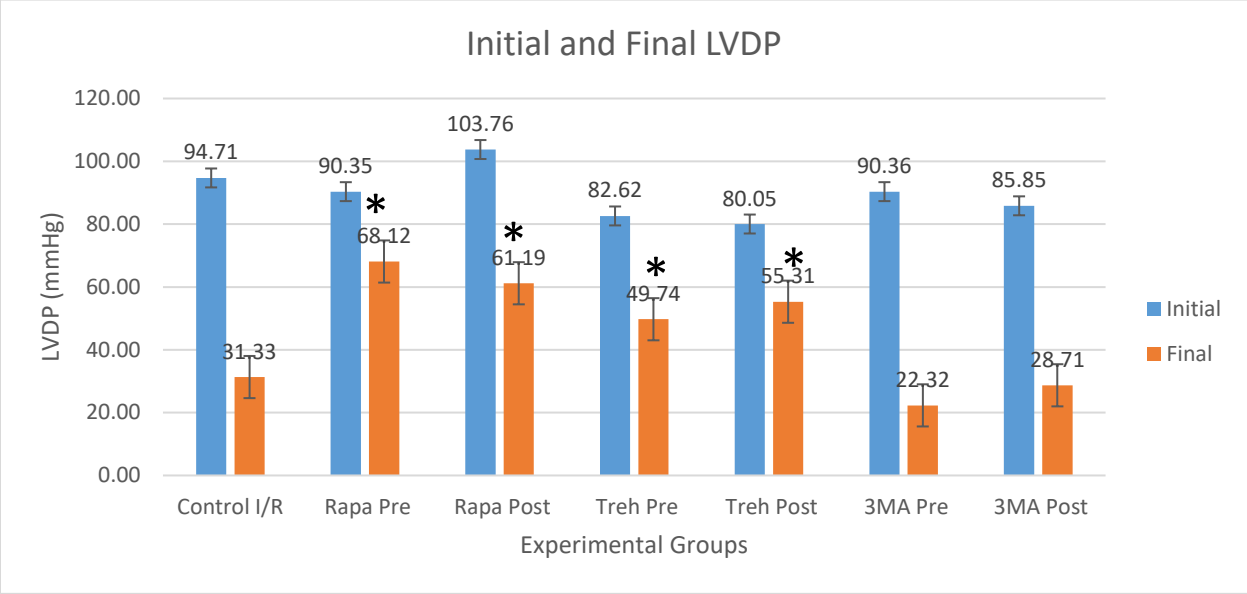

Figure 20a. Initial and final LVDP values of control I/R, autophagy enhancement groups, and autophagy inhibitor groups. Asterisk (*) indicates significance compared to final control I/R group.

Time course of LVDP for control I/R and both rapamycin treatment groups are illustrated in Figure 20b. The control I/R group showed dramatically compromised LVDP at 5 minutes (11.5 ± 13.0 mmHg) compared to its initial value (94.7 ± 10.4 mmHg). Then the LVDP level began to rise throughout the reperfusion time but never returned to its initial value. At the end of the reperfusion, the control I/R LVDP was 31.3 ± 18.9 mmHg. Moreover, both rapamycin treatments had initially compromised LVDP levels but improved faster compared to control I/R. However, rapamycin pre-treatment significantly improved LVDP from 20 to 45 minutes of reperfusion when compared to control I/R (all $p<0.05$). Rapamycin post-treatment only showed significantly improved LVDP at 45 minutes reperfusion. Additionally, rapamycin pre-treatment showed significantly higher LVDP at 5, 10, 20, 25, and 30 minutes reperfusion when compared to rapamycin post-treatment ($p<0.05$).

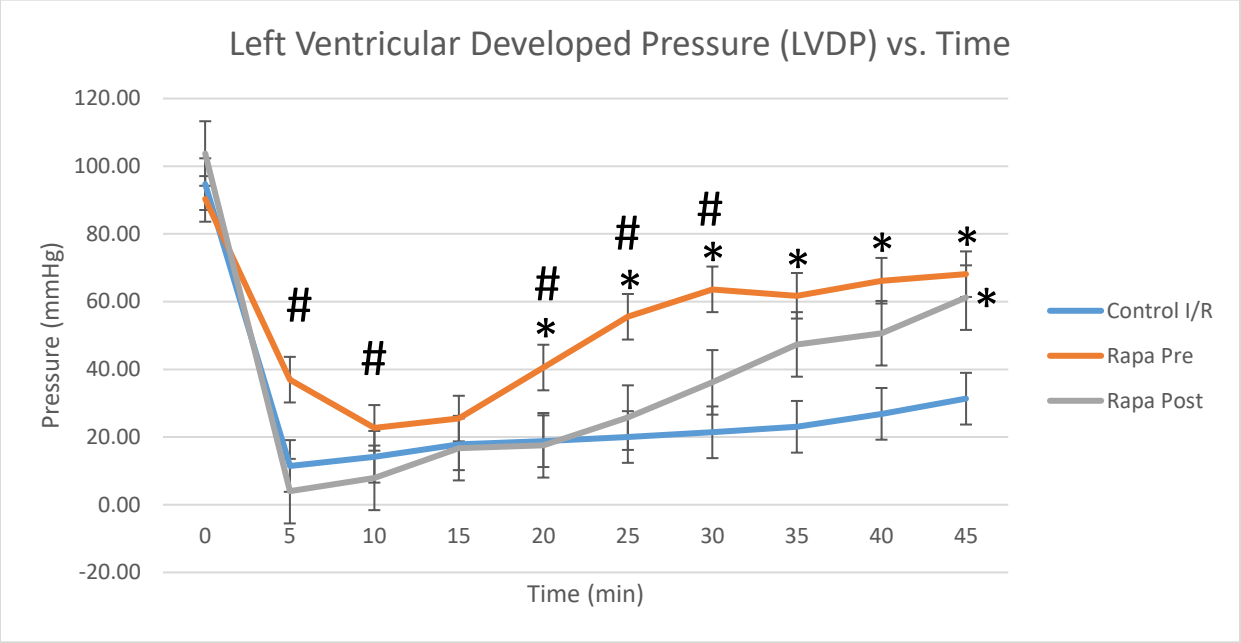

Figure 20b. Time course of rapamycin LVDP. Asterisk (*) indicates significant difference between either rapamycin treatment groups when compared to control I/R. Hashtag (#) indicates significant difference when rapamycin pre-treatment is compared to rapamycin post-treatment.

Time course of LVDP for control I/R and both trehalose treatment groups are illustrated in Figure 20c. Compared to the control I/R group, trehalose pre and post-treatment showed initially compromised LVDP values at 5 minutes (13.3 ± 10.7 mmHg and 21.9 ± 16.7 mmHg, respectively) compared to their initial values (82.6 ± 9.0 mmHg and 80.1 ± 19.4 mmHg, respectively), and began to rise throughout the reperfusion period. Trehalose post-treatment, not pre-treatment, showed significantly improved LVDP values at 10, 25, 30, and 45 minutes of reperfusion when compared to control I/R. Additionally, trehalose pre-treatment showed significantly improved LVDP value at 10 minutes of reperfusion when compared to trehalose post-treatment.

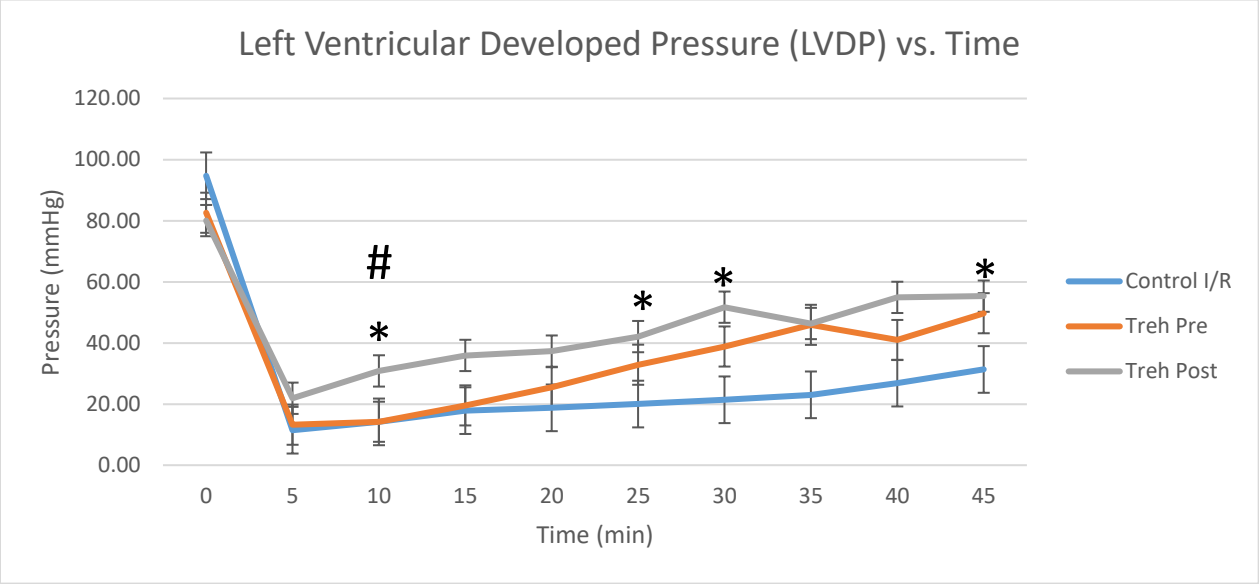

Figure 20c. Time course of trehalose LVDP. Asterisk (*) indicates significant difference between either trehalose treatment groups when compared to control I/R. Hashtag (#) indicates significant difference when trehalose pre-treatment is compared to trehalose post-treatment.

By contrast, trehalose pre-treatment showed significantly improved LVDP at 25 and 30 minutes of reperfusion when compared to rapamycin pre-treatment (both $p<0.05$). Trehalose post-treatment showed a significantly improved LVDP at 10 minutes of reperfusion when compared to rapamycin post-treatment at the same time ($p<0.05$). Autophagy inhibitor group time points were not included because there was no significance of LVEDP when compared to control I/R group at any time point.

3.4 Maximum Rate of Pressure Change (+dP/dT max)

Initial dP/dT max among all groups were similar and control I/R group showed a very low final dP/dT max level. By contrast, autophagy enhancement as pre or post-treatment showed an improved rate of pressure change when compared to final control I/R. Rapamycin pre-treatment showed the highest dP/dT max level ($p<0.05$). However, autophagy inhibition as pre or post-

treatment did not significantly change final dP/dT max when compared to control I/R (Figure 21a).

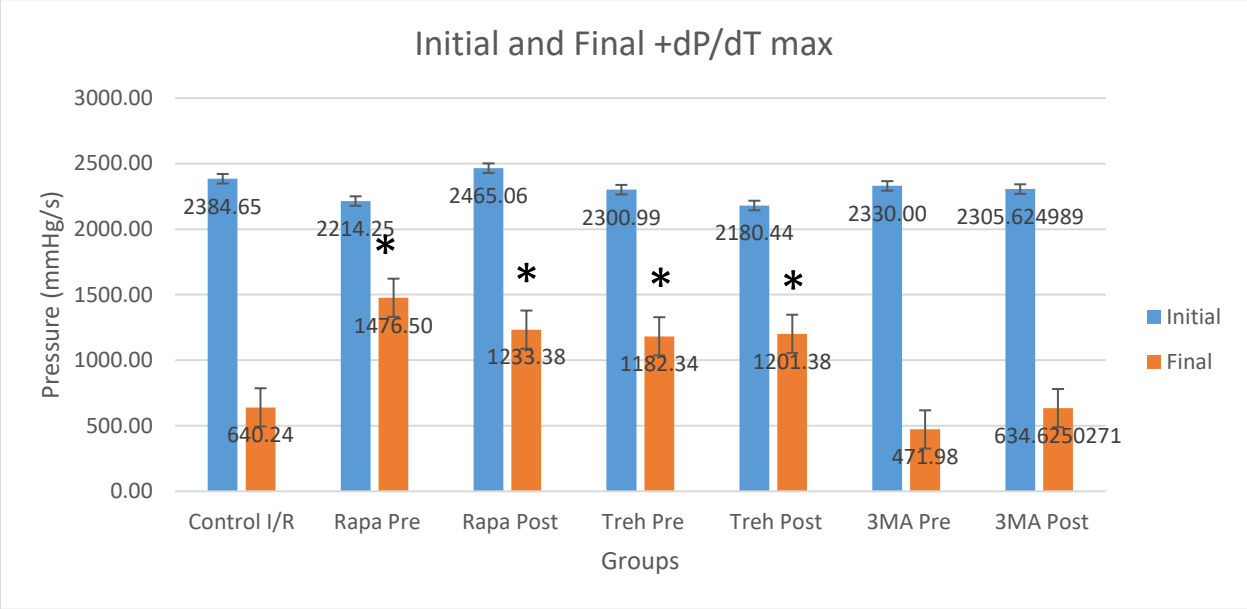

Figure 21a.Initial and final dP/dT max values of control I/R, autophagy enhancement groups, and autophagy inhibitor groups. Asterisk (*) indicates significance compared to final control I/R group.

Time course of dP/dT max for control I/R and both rapamycin treatment groups are illustrated in Figure 21b. The control I/R group showed a dramatically compromised of dP/dT max at 5 minutes (695.5 ± 431.6 mmHg/s) compared to its initial value (2214.3 ± 407.0 mmHg/s). Then the dP/dT max levels began to rise and remained relatively constant throughout the reperfusion time but never returned to its initial value. At the end of reperfusion, the dP/dT max for the control I/R was 640.2 ± 313.6 mmHg/s. Moreover, both rapamycin treatments had initially compromised dP/dT max levels but improved faster afterwards. However, rapamycin pre-treatment, significantly improved dP/dT max from 25 to 45 minutes of reperfusion when

compared to control I/R. Rapamycin post-treatment significantly improved dP/dT max levels at 45 minutes of reperfusion. Rapamycin pre-treatment showed significance occurred at more time points than did rapamycin post-treatment. Additionally, rapamycin pre-treatment showed significantly improved dP/dT max levels at 25, 30, 35, and 40 minutes of reperfusion when compared to rapamycin post-treatment ($p<0.05$).

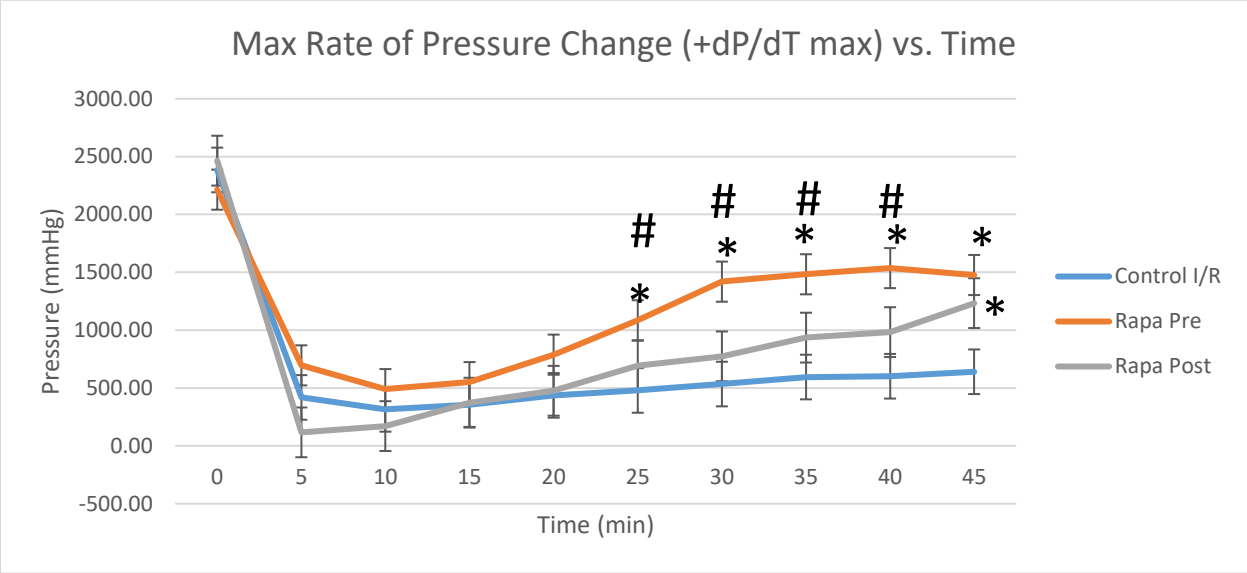

Figure 21b. Time course of rapamycin dP/dT max. Asterisk (*) indicates significant difference between either rapamycin treatment groups when compared to control I/R. Hashtag (#) indicates significant difference when rapamycin pre-treatment is compared to rapamycin post-treatment.

Time course of dP/dT max for control I/R and both trehalose treatment groups are illustrated in Figure 21c. Compared to the control I/R group, trehalose pre and post-treatment followed a similar trend of initially having compromised dP/dT max values at 5 minutes (282.1 ± 229.9 mmHg/s and 399.2 ± 198.6 mmHg/s, respectively) compared to their initial values (2301.0 ± 227.4 mmHg/s and 2180.4 ± 494.6 mmHg/s, respectively), but then the dP/dT max values began

to improve. Trehalose pre-treatment only showed significantly improved dP/dT max at 45 minutes of reperfusion, while trehalose post-treatment showed significantly improved dP/dT max at 20, 25, 30, and 45 minutes of reperfusion ($p<0.05$). Trehalose post-treatment showed significance occurring at more time points than did trehalose pre-treatment. Additionally, trehalose post-treatment showed significantly improved dP/dT max levels at 20 and 25 minutes of reperfusion when compared to trehalose pre-treatment ($p<0.05$). Autophagy inhibitor group time points were not included because there was no significance of dP/dT max when compared to control I/R group at any time point.

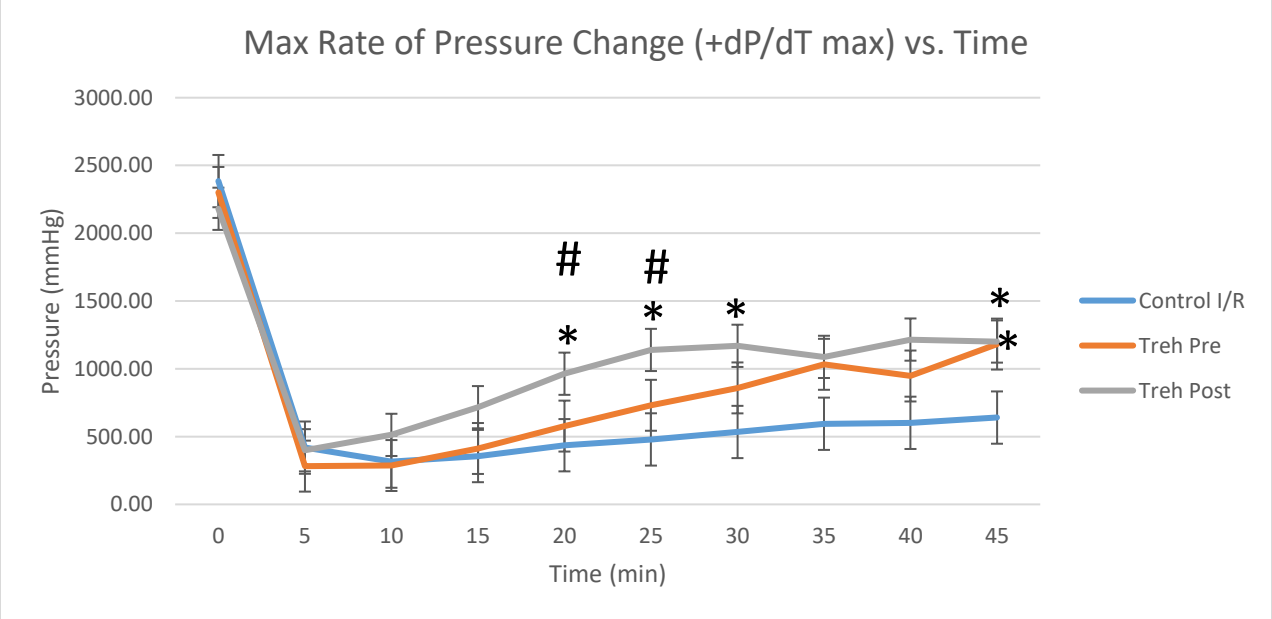

Figure 21c. Time course of trehalose dP/dT max. Asterisk (*) indicates significant difference between either trehalose treatment groups when compared to control I/R. Hashtag (#) indicates significant difference when trehalose pre-treatment is compared to trehalose post-treatment.

Note, rapamycin pre-treatment showed significantly improved dP/dT max levels at 20, 25, 30, and 40 minutes of reperfusion when compared to trehalose pre-treatment. However, no significance occurred in comparison of post-treatment groups.

3.5 Minimum Rate of Pressure Change (-dP/dT min)

Initial dP/dT min among all groups were similar and control I/R group showed compromised dP/dT min level. By contrast, autophagy enhancement as pre or post-treatment showed significantly improved rate of pressure change when compared to final control I/R ($p<0.05$). However, autophagy inhibition as pre or post-treatment did not show a significant change in final dP/dT min when compared to final control I/R (Figure 22a).

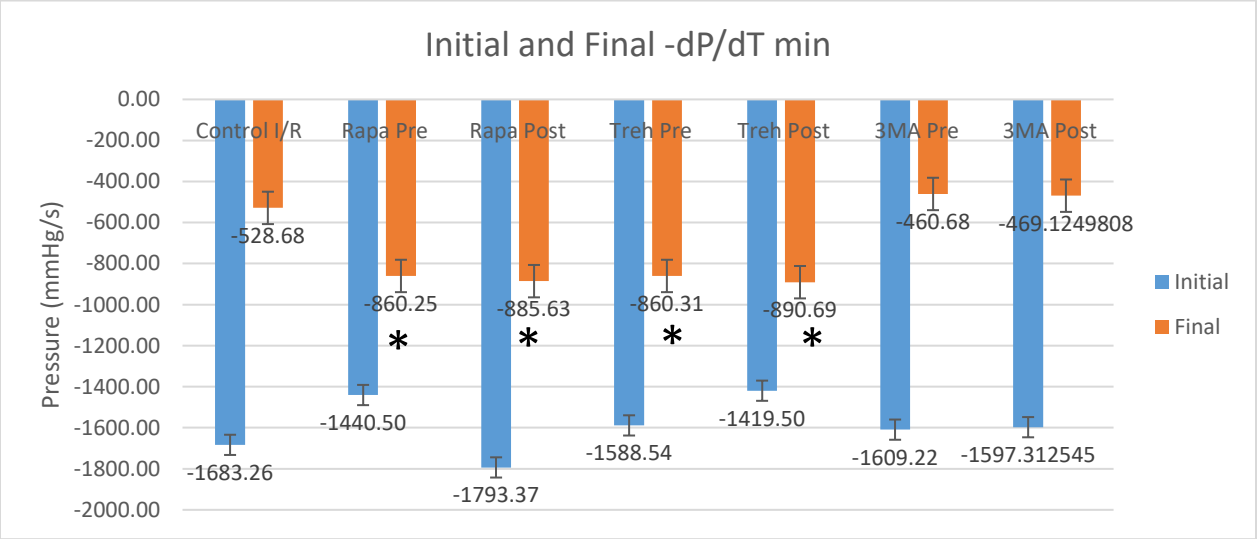

Figure 22a. Initial and final dP/dT min values of control I/R, autophagy enhancement groups, and autophagy inhibitor groups. Asterisk (*) indicates significance compared to final control I/R group.

Time course of dP/dT min for control I/R and both rapamycin treatment groups are illustrated in Figure 22b. The control I/R group showed dramatically compromised dP/dT min at 5 minutes (-577.3 ± 293.2 mmHg/s) compared to its initial value (-1440.5 ± 402.3 mmHg/s). Then the

absolute dP/dT min value remained relatively constant throughout the reperfusion time but never returned to its initial value. The final dP/dT min value for the control I/R at the end of reperfusion was -528.7 ± 208.9 mmHg/s. Moreover, both rapamycin treatments had initially compromised dP/dT min values as well. However, rapamycin pre-treatment, not rapamycin post-treatment, significantly improved dP/dT min at 5, 25, 30, 35, and 45 minutes of reperfusion when compared to control I/R ($p<0.05$). Additionally, rapamycin pre-treatment showed significantly improved dP/dT min values at 5 and 25 minutes of reperfusion when compared to rapamycin post-treatment ($p<0.05$).

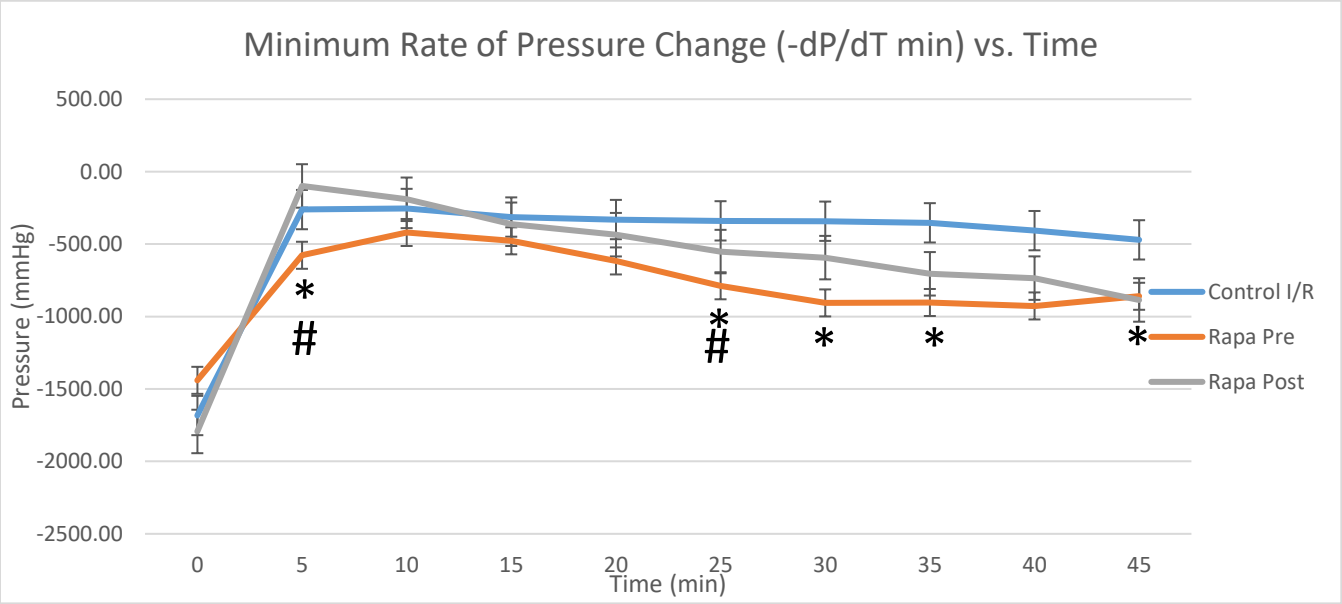

Figure 22b. Time course of rapamycin dP/dT min. Asterisk (*) indicates significant difference between either rapamycin treatment groups when compared to control I/R. Hashtag (#) indicates significant difference when rapamycin pre-treatment is compared to rapamycin post-treatment.

Time course of dP/dT min for control I/R and both trehalose treatment groups are illustrated in Figure 22c. Compared to the control I/R group, trehalose pre and post-treatment followed a

similar trend of initially having compromised dP/dT min values at 5 minutes (-229.4 ± 166.9 mmHg/s and -201.7 ± 54.4 mmHg/s, respectively) compared to their initial values (-1588.5 ± 230.2 mmHg/s and -1419.5 ± 341.4 mmHg/s, respectively), but then the absolute dP/dT min values began to improve. Trehalose pre-treatment only showed significantly improved dP/dT min at 45 minutes of reperfusion, while trehalose post-treatment showed significantly improved dP/dT min at 20, 25, and 30 minutes of reperfusion when compared to control I/R ($p<0.05$). Trehalose post-treatment showed significance occurring at more time points than did Trehalose pre-treatment. Autophagy inhibitor group time points were not included because there was no significance of -dP/dT min when compared to control I/R group at any time point.

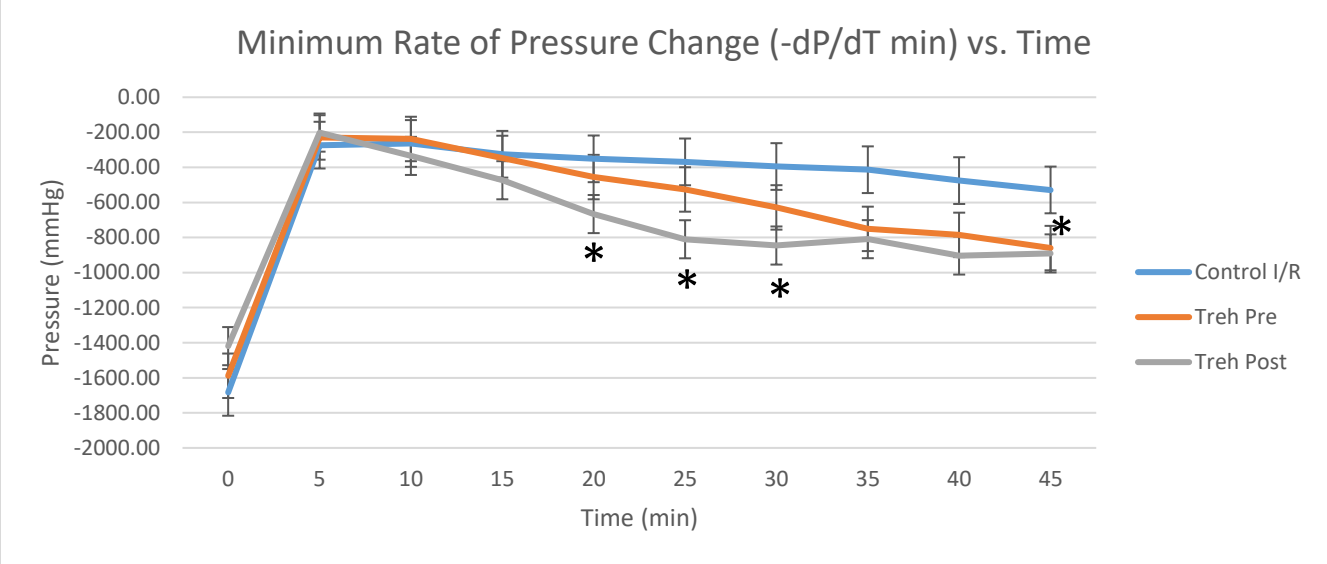

Figure 22c. Time course of trehalose dP/dT min. Asterisk (*) indicates significant difference between either trehalose treatment groups compared to control I/R.

3.6 Heart Rate (HR)

Initial HR among all groups were similar and the control I/R showed a slight increase in the final HR. By contrast, both rapamycin and trehalose pre-treatment and post-treatment groups,

as well as 3-MA post-treatment, all showed a slight decrease in the final HR when compared to control I/R group. However, 3-MA pre-treatment did show an increase in the final HR when compared to the control I/R. In summary, the initial and final HR among different groups were not statistically significant (Figure 23).

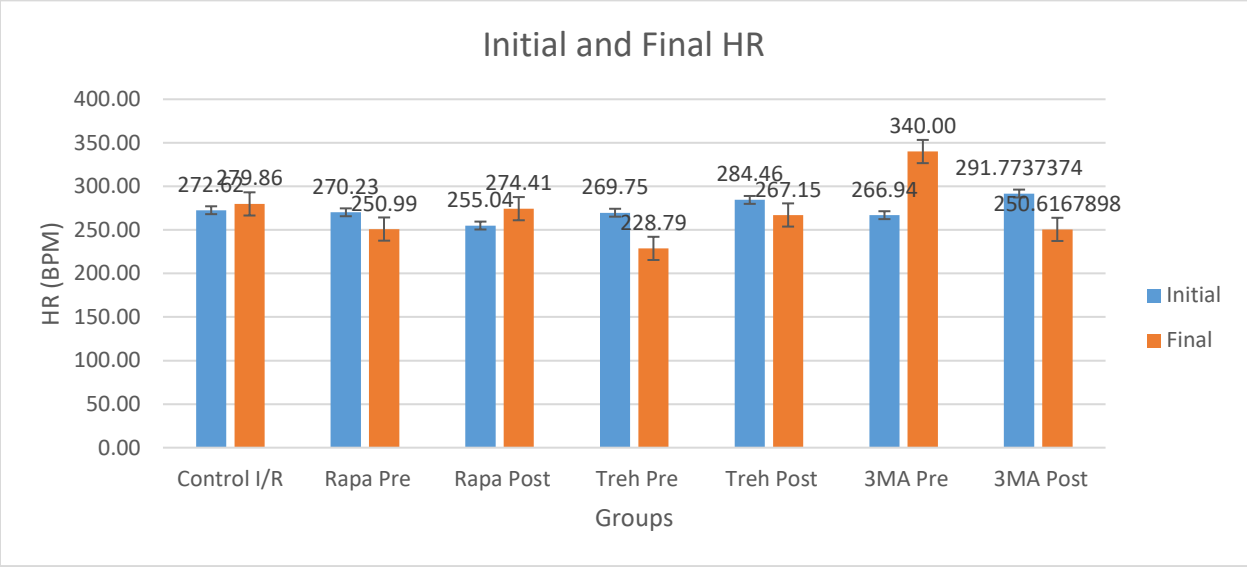

Figure 23. Initial and final heart rate values of control I/R, autophagy enhancement groups, and autophagy inhibitor groups showed no significant change when compared to each other.

3.7 Coronary Flow (CF)

The initial CF between all groups were within the standard deviation of the standard mean with control I/R showing a significant decrease in the final CF. Both autophagy enhancement and inhibitor groups showed a similar pattern in the decrease in final CF when compared to their respective initial values. There was no significant change between any of the groups. In summary, the initial and final CF among different groups were not statistically significant. (Figure 24a).

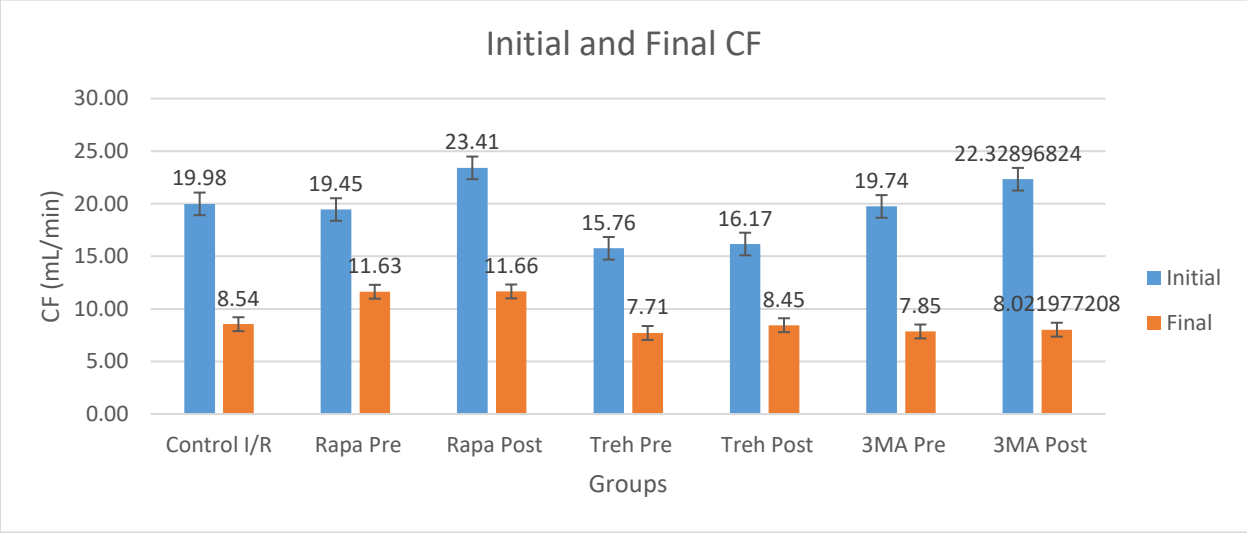

Figure 24a. Initial and final coronary flow values of control I/R, autophagy enhancement groups, and autophagy inhibitor groups.

Time course of coronary flow for control I/R and both rapamycin treatment groups are illustrated in Figure 24b. The control I/R group showed a dramatic decrease in the coronary flow at 5 minutes (7.7± 2.3 mL/min) compared to its initial value (20.0 ± 6.4 mL/min). Then the coronary flow remained relatively constant throughout the reperfusion time but never returned to its initial value. The final coronary flow of the control I/R was 8.5 ± 2.6 mL/min. Moreover, both rapamycin treatments had compromised coronary flow levels as well when compared to their initial values. However, rapamycin pre-treatment significantly improved coronary flow at 30 and 45 minutes of reperfusion when compared to control I/R, while rapamycin post-treatment only showed significantly improved CF at 30 minutes into reperfusion ($p<0.05$).

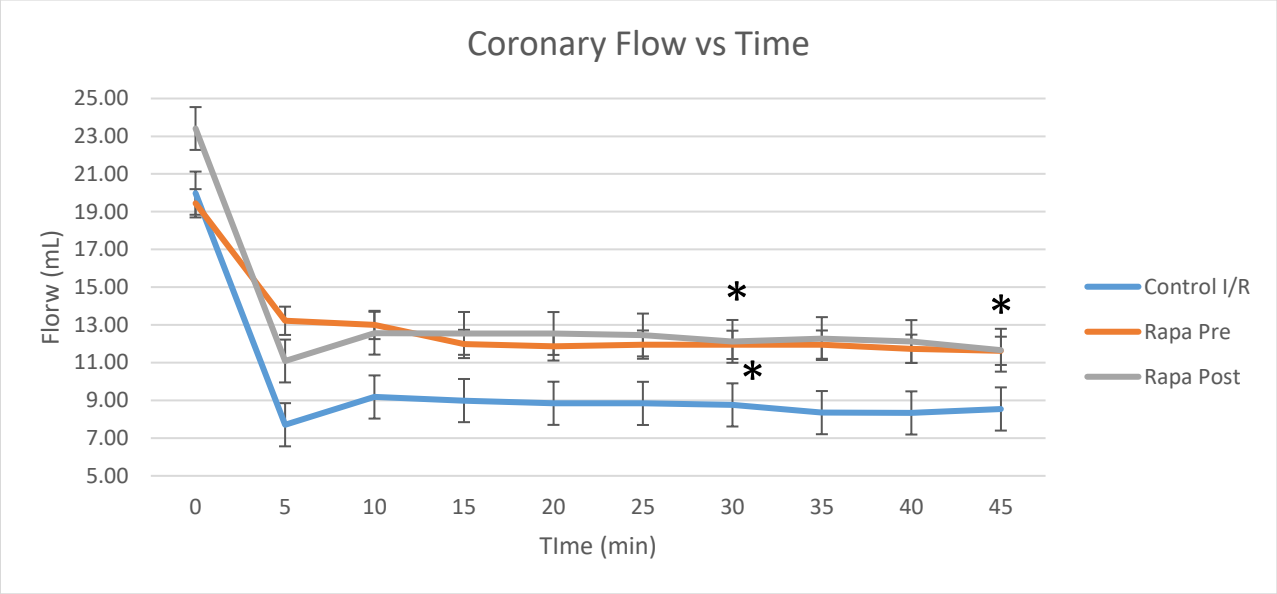

Figure 24b. Time course of rapamycin coronary flow. Asterisk (*) indicates significant difference between either rapamycin treatment groups when compared to control I/R.

Time course of coronary flow for control I/R and both trehalose treatment groups are illustrated in Figure 24c. Compared to the control I/R group, trehalose pre and post-treatment followed a similar trend of initially compromised coronary flow at 5 minutes (8.1± 2.2 mL/min and 5.5 ± 3.2 mL/min, respectively) compared to their initial values (15.8 ± 4.1 mL/min and 16.2 ± 3.2 mL/min, respectively), and remained constant. Trehalose pre and post-treatment did not show significance at any time during reperfusion when compared to control I/R. However, rapamycin pre-treatment showed significantly improved coronary flow at 30 minutes of reperfusion when compared to trehalose pre-treatment ($p<0.05$). Additionally, rapamycin post-treatment also showed significantly improved coronary flow only at 5 minutes of reperfusion when compared to trehalose post-treatment ($p<0.05$).

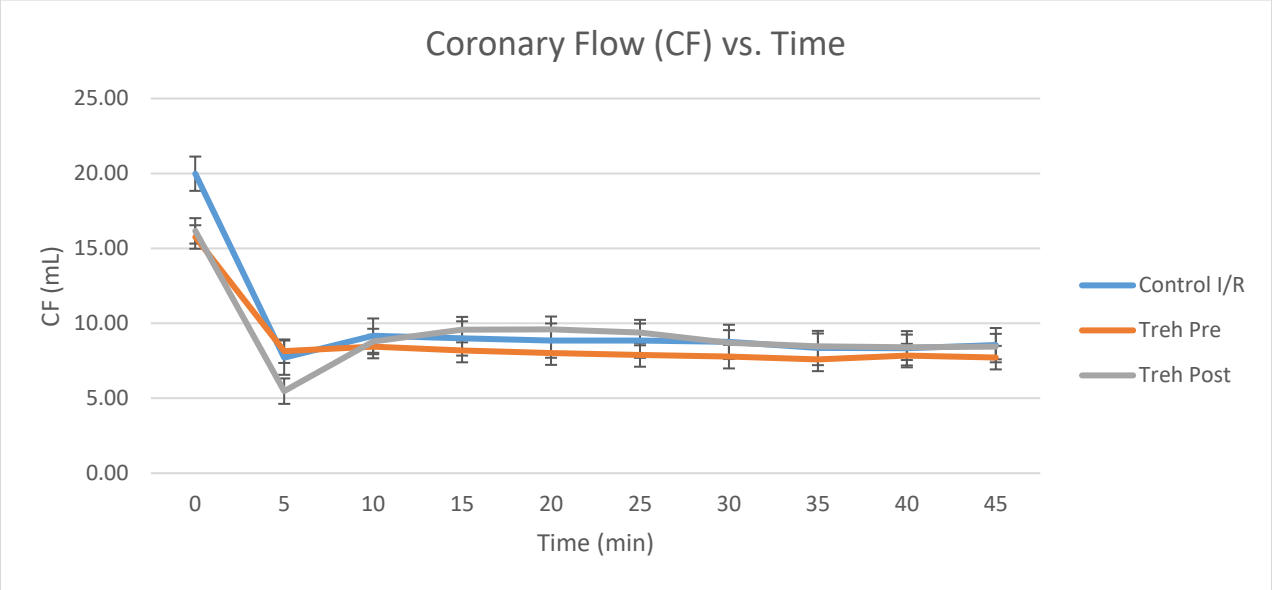

Figure 24c. Time course of trehalose coronary flow.

3.8 Cardiac Infarction Size

Pictures of infarct size for each group were also included. The control I/R showed a relatively large white ring of dead cardiomyocytes on the edge of the cross-sectional slice. Autophagy inhibitor groups showed a similar trend to control I/R in terms of a big infarct size. However, autophagy enhancement groups were not similar to control I/R. Both autophagy enhancement groups showed smaller white ring size surrounding the heart, indicating that the infarct size has been reduced (Figure 25a).

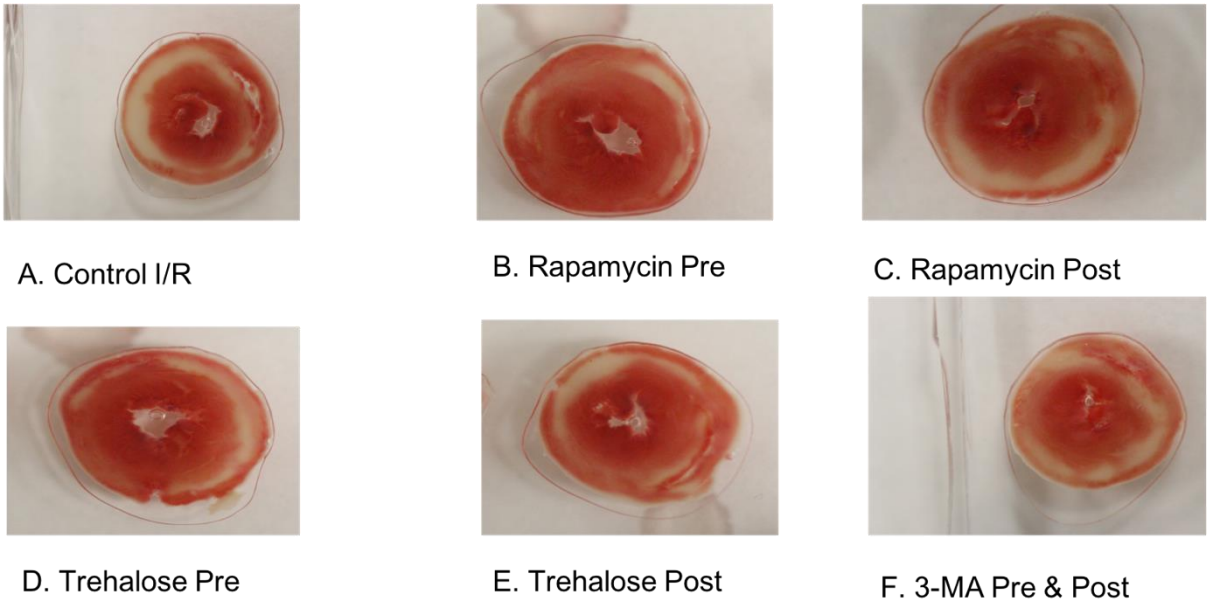

Figure 25a. Representative cross-sectional slices of infarcted study groups

Quantitatively, control I/R had a high infarct percentage of 39 ± 4%. By contrast, autophagy enhancement as pre or post-treatment showed a significant decrease in infarct percentage compared to control I/R ($p<0.05$). Rapamycin pre-treatment had the lowest infarct percentage. Autophagy inhibition as pre or post-treatment also showed a similar infarct percentage as control I/R (Figure 25b).

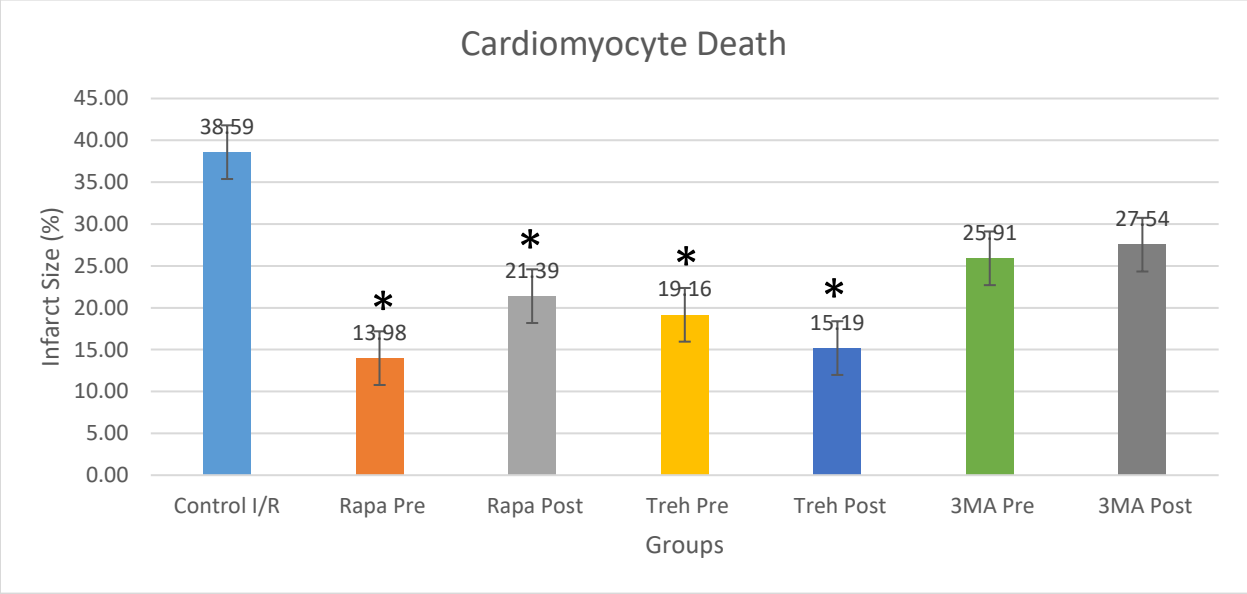

Figure 25b. Qualitative representation of cardiomyocyte death among all study groups

DISCUSSION

4.1 Summary of Findings

The results of this study showed that the control I/R isolated heart had compromised cardiac function as can be seen by a significant increase in LVEDP, a decrease in LVDP, decreased rate of pressure change (i.e. dP/dT max and min), dramatically decreased coronary flow, and a high infarct size. The autophagy inhibitor, 3-methyladenine, given as either pre or post-treatment also showed similar results to the control I/R in terms of compromised cardiac function and increased infarct size. However, these results also confirmed that autophagy enhancement by both rapamycin and trehalose, as either pre or post-treatment, are beneficial to cardiac function with significant improvement in LVEDP, LVDP, and dP/dT max and min values when compared to control I/R. The autophagy enhancer-treated hearts showed a significant reduction in infarct size when compared to the control I/R.

4.1.1 Control I/R

The Langendorff heart preparation maintained normal cardiac parameters under perfusion of krebs buffer; the range of cardiac parameters for the Langendorff preparation are: heart rate was 272.5 ± 6.2 bpm, LVEDP was 9.4 ± 3.1 mmHg, LVDP was 95.3 ± 10.1 mmHg, dP/dT max was 2413.7 ± 236.3 mmHg/s, and dP/dT min was -1712.1 ± 327.2 mmHg/s. The Langendorff preparation has been widely used to induce ischemia and reperfusion injury by decreasing cardiac function and increasing infarct size (Doring, 1990). After induction of ischemia and reperfusion, the cardiac parameters were as follows: heart rate was 255.3 ± 34.3 bpm, LVEDP was 66.6 ± 7.0 mmHg, LVDP was 33.3 ± 16.5 mmHg, dP/dT max was 640.2 ± 313.6 mmHg/s,

and dP/dT min was -528.7 ± 208.9 mmHg/s. Another study using the Langendorff preparation to monitor cardiac function before and after I/R also showed similar compromised cardiac function and increased infarct size to our own preparation, however, ischemia was induced for 30 minutes and reperfusion for 90 minutes (Luan, 2012).

Reduced cardiac function during I/R is principally caused by cellular disturbances during I/R. During ischemia ATP production decreases because of a lack of oxygen. This forces the cardiomyocyte to switch from aerobic to anaerobic respiration and decreases oxidative phosphorylation needed for ATP synthesis (Hausenloy & Yellon, 2013). Moreover, anaerobic respiration leads to increased acidity within the cell and the mitochondria becomes damaged. Any ATP already made in the cell before the ischemic period is broken down to maintain the mitochondrial membrane potential. The lack of ATP during ischemia also causes the Na/K ATPase to stop, thus, causing intracellular Na to increase since the Na-H exchanger has already been activated in response to acidic levels in the cardiomyocyte. To rid the cell of the excess Na, the Na-Ca exchanger is activated, causing calcium in the cytosol to increase and overload the cell.

During reperfusion, a burst of free radical production occurs from multiple sources; in particular, from the mitochondria. Normally, mitochondria produce ATP by moving protons from complexes 1, 3, and 4 in the ETC and producing oxygen that is then reduced to water (Ray, 2013). However, in the production of ROS, the oxygen molecule is not fully reduced and forms into a superoxide or free radical (Ray, 2013). When the mitochondria have been damaged it does not produce as much ATP, and along with the decrease in ATP production the isolated heart suffers from a calcium overload due to damage of the sarcoplasmic reticulum (SR) by ROS and

the calcium brought in during ischemia, thus relatively maintaining LVESP and increasing LVEDP values (Hausenloy & Yellon, 2013).

The ROS also contributes to cell damage by activating different apoptotic pathways that allow cytochrome c to leak out of the mitochondria and ultimately increase the infarct size of the isolated heart. An increase in infarct inversely correlates to a decrease in cardiac function, which may also explain why our results showed compromised cardiac values (Mathey, 1974). Our infarct size was 38.6 ± 12.7 % and was very similar to previous studies (Luan, 2012).

Along with the increase in ROS, insufficient ATP production can also compromise Ca-ATPase at the SR and cell membrane and reduce the amount of calcium to be removed from the cytosol in order to properly allow the ventricles to relax. Normally, calcium depends on concentration gradients for entry and exit of a cell, and this is done by either the Ca-ATPase or the Na-Ca exchanger, as previously mentioned. However, in order for the Ca-ATPase to work it requires ATP, which is present at very low levels during reperfusion, therefore, only small amounts of calcium are removed (McDowall,). Without ATP to activate the Ca-ATPase and decrease calcium concentrations, the LVESP remains high, while the hyper contractile activity of the heart prevents the LVEDP from getting low enough to allow the ventricles to be filled with blood.

This calcium overload also contributes to the low final LVDP values because it prevents LVEDP from getting to low enough values to make a difference in the pressure needed to pump blood out into systemic circulation. Note, the excess calcium and decreased ATP production compromised the rate of pressure change (e.g. dP/dT max and min) because without ATP the

rate of contraction and relaxation reduces and ultimately effects perfusion of the coronary arteries.

Finally, coronary flow was reduced by approximately 55% in the control I/R group. The initial flow was 20.1 ± 6.2 mL/ min and the final flow was 8.5 ± 2.7 mL/min. Constant pressure was used to perfuse the isolated heart, therefore, reduction of coronary flow indicated increased vascular resistance (Flow=change in pressure/resistance). Normally, coronary blood vessels dilate due to NO derived from endothelial cells. However, ROS overproduction during reperfusion will decrease the amount of endothelial cells available to stimulate vasodilation and ultimately allows vasoconstriction to persist. Meanwhile, abnormal ion distribution, specifically Na and Ca, will cause the cell to swell and press up against the blood vessels. This swelling will also contribute in the reduction of blood flow, oxygen, and nutrients that will be available to heart, thus decreasing cardiomyocyte function, and negatively impacting other organ systems since the heart cannot send enough blood into systemic circulation.

4.1.2 Drug Treatments

4.1.2.1 Autophagy Enhancers

Results indicated that autophagy enhancement as either pre-treatment or post-treatment provided cardioprotective effects by improving cardiac function and decreasing infarct size compared to the control I/R group. The enhancement of autophagy is able to be beneficial to the heart by increasing ATP and decreasing ROS production and does so by removing damaged mitochondria. This specialized process of autophagy dealing with mitochondria is known as

mitophagy. By removing the damaged mitochondria, autophagy is able to decrease the rate of ROS produced and increase the amount of ATP by allowing the undamaged mitochondria to remain within the cell and carry out their normal function.

Andres et al. found that mitophagy is needed for cardio protection by using the drug simvastatin in a pre-treatment in-vivo and in-vitro rat model (Andres, 2014). Their results showed that simvastatin-treated cardiomyocytes exhibited mitochondrial translocation of PARKIN, a ubiquitin ligase used to specifically target damaged mitochondria for autophagy/mitophagy, promoted a decrease in infarct size (Andres, 2014). Andres et al. also confirmed that simvastatin's cardioprotective role was dependent on PARKIN-mediated mitophagy by inhibiting PARKIN translocation and recorded increased infarction compared to their control group.

4.1.2.1.1 Rapamycin Pre and Post-treatment

A previous study found that rapamycin when given as pre-treatment has cardioprotective characteristics, as can be seen by a decrease in infarct size and an increase in LVDP and coronary flow. This study suggested that by activating PI3 kinase-Akt pathway and mitochondria K-ATP channels in rats, rapamycin was able to be beneficial to cardiac function (Yang, 2010). Moreover, they used western blot analysis and immunostaining to check for an autophagic flux marker, LC3-2, in both non-treated (i.e., control) and treated groups (rapamycin pre-treatment). They found that rapamycin pre-treatment showed an increase in LC3-2 compared to the control (Yang, 2010). In this study, the optimal dose was 2mg/kg in DMSO, thus, the concentration of rapamycin in the rat was 24uM, assuming that the blood volume was 25mL. The concentration of rapamycin used in our study was 25nM given as either pre or post-treatment. We think that

because they administered rapamycin in vivo, the concentration of rapamycin in the heart was greatly affected by the pharmacokinetics of the drug. By contrast, we directly infused rapamycin into the isolated heart (i.e. ex-vivo).

A different study done by Filippone et al. also confirmed that rapamycin is involved with opening the mitochondrial ATP-sensitive K channels during pre-treatment but discussed how autophagy enhancement during post-treatment involves another route that specifically occurs during reperfusion and deals with Reperfusion Injury Salvage Kinases (RISK) (Yang, 2010). They discovered that RISK pathway works by avoiding the opening of the mitochondrial permeability transition pore and phosphorylates the salvage kinases AKT/mTORC2 and ERK.

Therefore, the way rapamycin is able to enhance autophagy may be a reason as to why rapamycin pre-treatment showed significantly improved cardiac function at certain parameters time points compared to rapamycin post-treatment. However, the infarct size between and cardiac function of both treatments were not significantly different.

4.1.2.1.2 Trehalose Pre and Post-treatment

Another drug used in our study was trehalose and we found that trehalose given as either pre or post-treatment also provided cardioprotective characteristics. Trehalose works independent of the mTOR pathway by increasing AMPK activity but not affecting mTOR activity. This was confirmed by Sarkar et al. where they found that the phosphorylation of downstream substrates of mTOR were unaffected by the introduction of trehalose (Belzile et al., 2016b). Trehalose blocks GLUT transporters allowing the cell to starve, thus slowing down metabolic activity and activating AMPK. Activation of AMPK induces autophagy by phosphorylating ULK-1, the mammalian homologue of Atg1. Multiple studies have shown that

trehalose is beneficial to cardio protection by functioning as an antioxidant or acting as a protein chaperone protecting against protein instability and denaturation (Mardones et al., 2016).

Sarkar et al. used 100mM of trehalose in mammalian cell culture and transfection lines, to examine its effects on various neurological diseases such as Parkinson's and Alzheimer's disease and found that trehalose enhanced autophagy and decreased protein aggregates by measuring LC3-2 to LC3-1 ratio and clearance of mutant proteins (Belzile et al., 2016). The trehalose concentration used in our study was 5mM and we found that trehalose post-treatment worked better than trehalose pre-treatment in terms of improved cardiac function and decreased infarct compared to each other. Post-treatment may be better because the antioxidant effects of trehalose would most likely be active during the reperfusion period since this is when ROS will be produced.

4.1.2.2 Autophagy inhibitor

3-MA is able to negatively impact autophagy enhancement by blocking class 3 PI3K, ultimately inhibiting Atg conjugation needed for the conversion of LC3-1 to LC3-2 to initiate autophagosome formation. Several studies have confirmed the downregulation of autophagy by determining the decreased LC3-2 levels in the presence of 3-MA using western blot and also noted the increase in infarct size compared to autophagy enhancement groups (Yang, 2010). One study found that using 10mM of 3-MA is sufficient for decreasing autophagy, however, we used 1mM concentration of 3-MA in our study because higher concentrations of 3-MA used in our Langendorff preparation showed significant and instant reduction of coronary flow and compromised cardiac function compared to control I/R.

4.2 Limitations of the Study

4.2.1 Isolated heart

The isolated heart did not duplicate the in-vivo situation since the heart is denervated and loses its ability to be influenced by the sympathetic or parasympathetic nervous systems, which play a central role in adapting to the metabolic needs of the body. For example, the normal heart rate for a rat ranges from 330-480 bpm, however, the heart rate for an isolated rat heart is 263 ± 5 bpm (Ijic, 1996). The heart rate for our control I/R group was 272.5 ± 16.9 bpm. Along with denervation, the isolated heart is just provided with glucose and no insulin in the Langendorff preparation via the krebs buffer. The lack of metabolic range can affect cardiac efficiency, contraction, and oxygen consumption (Aksentijevic, 2015).

The Langendorff preparation itself also provided limitations to the isolated heart. First, the Langendorff preparation is mostly used for small animals such as rats and rabbits and is not used for larger animals because of increasing complexity in the organism (Schetcher, 2014). Because of the lack of translation between bigger and smaller animals, clinically relevant isolated hearts are not used often (Schetcher, 2014).

4.2.2 Global ischemia

By putting the heart into global ischemia, the entire heart is negatively affected by this induction of ischemia and increases the number of damaged cardiomyocytes. An increase in the number of dead cardiomyocytes means that cardiac function will also be negatively affected. However, this may not be the case for when the heart suffers from regional ischemic episodes since the entire heart is not being affected.

The clinical correlation of global I/R is heart transplantation. In order for our study to mimic the effects of what an individual suffers from in a heart attack, the best way would be to induce some type of partial ischemia.

4.3 Future Studies

1. Evaluate autophagy influx index, such as LC3-2 and Beclin-1 from heart tissue harvested after experiments. Multiple studies have shown that LC3-2 and Beclin-1 levels are increased in autophagy enhancement when analyzed using western blot or immunofluorescence (Luan, 2012). This is to ensure that the cardioprotective effects attributed by the autophagy enhancers is actually due to an increase in autophagy.

2. Evaluate the change of the autophagy induction markers by measuring LC3-2 and Beclin-1 in an isolated hypoxia/re-oxygenation cardiomyocyte model. Once the cardiomyocyte extraction protocol has shown to provide consistently moderate to high yields of rod-shaped cardiomyocytes under the microscope, then introduction of the autophagy enhancer and inhibitor as either pre or post-treatment will be analyzed by the autophagic flux markers to confirm the previously stated hypothesis.

3. Evaluate the effects of autophagy enhancers or inhibitors in isolated hypoxia/ re-oxygenation cardiomyocytes model.

REFERENCES

AHA. (a). Acute coronary syndrome. Retrieved from http://www.heart.org/HEARTORG/Conditions/HeartAttack/AboutHeartAttacks/Acute-Coronary-Syndrome_UCM_428752_Article.jsp#.Wx7Dni-ZNsN

AHA. (b). Heart disease and stroke statistics 2017. Retrieved from https://healthmetrics.heart.org/wp-content/uploads/2017/06/Heart-Disease-and-Stroke-Statistics-2017-ucm_491265.pdf

AHA Staff. (2017). What is cardiovascular disease. Retrieved from http://www.heart.org/HEARTORG/Conditions/What-is-Cardiovascular-Disease_UCM_301852_Article.jsp#.Wx69ay-ZPR1

Aksentijevic, D. e. a. (2015). Is rate–pressure product of any use in the isolated rat heart? assessing cardiac 'effort' and oxygen consumption in the langendorff-perfused heart. *The Physiological Society*, Retrieved from https://physoc.onlinelibrary.wiley.com/doi/full/10.1113/EP085380

Andres, A. e. a. (2014). Mitophagy is required for acute cardioprotection by simvastatin. *Forum Original Research Communication*,

Argosy.Circulatory pulmonary & systemic circulation. Retrieved from https://www.visiblebody.com/learn/circulatory/circulatory-pulmonary-systemic-circulation

Ballou, L., & Lin, R. (2008). Rapamycin and mTOR kinase inhibitors *Journal of Chemical Biology,* Retrieved from https://www.ncbi.nlm.nih.gov/pmc/articles/PMC2698317/

Belzile, J., Sabalza, M., Craig, M., Clark, E., Morello, C. S., & Spector, D. H. (2016a). Trehalose, an mTOR-independent inducer of autophagy, inhibits human cytomegalovirus infection in multiple cell types. *Journal of Virology, 90*(3), 1259-1277. 10.1128/JVI.02651-15 Retrieved from http://www.ncbi.nlm.nih.gov/pubmed/26559848

Belzile, J., Sabalza, M., Craig, M., Clark, E., Morello, C. S., & Spector, D. H. (2016b). Trehalose, an mTOR-independent inducer of autophagy, inhibits human cytomegalovirus infection in multiple cell types. *Journal of Virology, 90*(3), 1259-1277. 10.1128/JVI.02651-15 Retrieved from http://www.ncbi.nlm.nih.gov/pubmed/26559848

Carol Chen-Scarabelli, Pratik R Agrawal. (2015). The role and modulation of autophagy in experimental models of myocardial ischemia-reperfusion injury . *Journal of Geriatric Cardiology,* , 338-348.

CDC.Heart disease facts. Retrieved from https://www.cdc.gov/heartdisease/facts.htm

Coronary artery disease types. Retrieved from https://my.clevelandclinic.org/health/diseases/16898-coronary-artery-disease/types

Doring, H. J.The isolated perfused heart according to langendorff technique--function--application.   Retrieved from https://www.ncbi.nlm.nih.gov/pubmed/2103635

Doring, H. J. (1990). The isolated perfused heart according to langendorff technique--function--application.   *Pub Med*, Retrieved from https://www.ncbi.nlm.nih.gov/pubmed/2103635

Hausenloy, D. J., & Yellon, D. M. (2013). Myocardial ischemia-reperfusion injury: A neglected therapeutic target. *The Journal of Clinical Investigation*, *123*(1), 92. 10.1172/JCI62874 Retrieved from http://www.ncbi.nlm.nih.gov/pubmed/23281415

Ijic, R.The isolated perfused “working” rat heart: A new method. *Journal of Pharmacological and Toxicological Methods*, Retrieved from https://www.sciencedirect.com/science/article/pii/1056871996000019

Ingwall, J. (2009). Energy metabolism in heart failure and remodelling *Cardiovascular Research*, Retrieved from https://www.ncbi.nlm.nih.gov/pmc/articles/PMC2639129/

Jean, Steve and Kiger, Amy. (2014). Classes of phosphoinositide 3-kinases at a glance *Pmc*, Retrieved from https://www.ncbi.nlm.nih.gov/pmc/articles/PMC3937771/

Kalogeris, T. e. a. (2014). Cell biology of ischemia/reperfusion injury *International Review of Cell and Molecular Biology*, Retrieved from https://www.ncbi.nlm.nih.gov/pmc/articles/PMC3904795/

Kang, R., Zeh, H., & Tang, D. (2011). The beclin 1 network regulates autophagy and apoptosis *Cell Death and Differentiation*, Retrieved from https://www.ncbi.nlm.nih.gov/pmc/articles/PMC3131912/

Klabunde, R. (2016). Cardiac cycle. Retrieved from http://www.cvphysiology.com/Heart%20Disease/HD002

Luan, H. e. a. (2012). Hydrogen sulfide postconditioning protects isolated rat hearts against ischemia and reperfusion injury mediated by the JAK2/STAT3 survival pathway. *Brazilian Journal of Medical and Biological Research*, Retrieved from https://www.ncbi.nlm.nih.gov/pmc/articles/PMC3854176/

Ma, S. e. a. (2014). The role of the autophagy in myocardial ischemia/reperfusion injury. *Biochimica Et Biophysica Acta (BBA) - Molecular Basis of Disease*, 10.1016/j.bbadis.2014.05.010 Retrieved from http://www.sciencedirect.com/science/article/pii/S0925443914001380?via%3Dihub

Manning, A., & Hearse, D. (1984). Reperfusion-induced arrhythmias: Mechanisms and prevention. *Journal of Cellular and Molecular Cardiology*, *16*(6) Retrieved from https://www.sciencedirect.com/science/article/pii/S0022282884806380

Mardones, P., Rubinsztein, D. C., & Hetz, C. (2016). Mystery solved: Trehalose kickstarts autophagy by blocking glucose transport. *Science Signaling*, *9*(416), fs2. Retrieved from http://www.ncbi.nlm.nih.gov/pubmed/26905424

Mathey, D. e. a. (1974). Attempt to quantitate relation between cardiac function and infarct size in acute myocardial infarction. *British Heart Journal*, Retrieved from http://heart.bmj.com/content/heartjnl/36/3/271.full.pdf

Mayo Clinic Staff. (a). Coronary heart disease. Retrieved from https://www.mayoclinic.org/diseases-conditions/coronary-artery-disease/symptoms-causes/syc-20350613

Mayo Clinic Staff. (b). Heart disease. Retrieved from https://www.mayoclinic.org/diseases-conditions/heart-disease/symptoms-causes/syc-20353118

McDowall, J.Calcium pumps

. Retrieved from https://www.ebi.ac.uk/interpro/potm/2004_3/Page1.htm

Mizushima, N. (2007). Autophagy: Process and function. *Genes & Development, 21*(22), 2861-2873. 10.1101/gad.1599207 Retrieved from http://www.ncbi.nlm.nih.gov/pubmed/18006683

Mozaffarian, D. e. a. (2015). Heart disease and stroke statistics 2016. *Circulation AHA,* Retrieved from http://circ.ahajournals.org/content/133/4/e38#sec-218

NIH.Coronary heart disease. Retrieved from https://www.nhlbi.nih.gov/health-topics/coronary-heart-disease

Nitroglycerin. Retrieved from https://www.healthline.com/health/nitroglycerin-sublingual-tablet#about

Przyklenk, K., Dong, Y., Undyala, V. V., & Whittaker, P. (2012). Autophagy as a therapeutic target for ischaemia /reperfusion injury? concepts, controversies, and challenges.

Cardiovascular Research, 94(2), 197-205. 10.1093/cvr/cvr358 Retrieved from http://www.ncbi.nlm.nih.gov/pubmed/22215722

Qi, D. (2015). AMPK: Energy sensor and survival mechanism in the ischemic heart *Trends in Endocrinology and Metabolism,* Retrieved from https://www.ncbi.nlm.nih.gov/pmc/articles/PMC4697457/

Ray, P. e. a. (2013). Reactive oxygen species (ROS) homeostasis and redox regulation in cellular signaling. *Pmc,* Retrieved from https://www.ncbi.nlm.nih.gov/pmc/articles/PMC3454471/

Rice University. (a). Anatomy & physiology. Retrieved from https://opentextbc.ca/anatomyandphysiology/chapter/19-2-cardiac-muscle-and-electrical-activity/

Rice University. (b). Anatomy and physiology. Retrieved from https://opentextbc.ca/anatomyandphysiology/chapter/19-1-heart-anatomy/

Richter, E. A., & Ruderman, N. B. (2009). AMPK and the biochemistry of exercise: Implications for human health and disease. *The Biochemical Journal*, *418*(2), 261. 10.1042/BJ20082055 Retrieved from http://www.ncbi.nlm.nih.gov/pubmed/19196246

Rui Sheng, & Zheng-hong Qin. (2015). The divergent roles of autophagy in ischemia and preconditioning. *Acta Pharmacologica Sinica*, *36*(4), 411. 10.1038/aps.2014.151 Retrieved from http://www.ncbi.nlm.nih.gov/pubmed/25832421

Schetcher, M. e. a. (2014). An isolated working heart system for large animal models *Journal of Visualized Experiments,* Retrieved from https://www.ncbi.nlm.nih.gov/pmc/articles/PMC4189428/

Serhiy Pankiv, Terje HÃ¸yvarde Clausen, Trond Lamark, Andreas Brech, Jack-Ansgar Bruun, Heidi Outzen, . . . Terje Johansen. (2007). p62/SQSTM1 binds directly to Atg8/LC3 to facilitate degradation of ubiquitinated protein aggregates by autophagy. *Journal of Biological Chemistry, 282*(33), 24131-24145. 10.1074/jbc.M702824200 Retrieved from http://www.jbc.org/content/282/33/24131.abstract

Sigma Aldrich.2,3,5-triphenyltetrazolium chloride. Retrieved from https://www.sigmaaldrich.com/catalog/product/sigma/t8877?lang=en&region=US

Sigma-Aldrich. (2017). 3-methyladenine autophagy inhibitor. Retrieved from http://www.sigmaaldrich.com/catalog/product/sigma/m9281?lang=en&region=US

Subodh Verma, Paul W.M. Fedak, Richard D. Weisel, Jagdish Butany, Vivek Rao, Andrew Maitland, Ren-Ke Li, Bikramjit Dhillon, Terrence M. Yau. (2002). Fundamentals of reperfusion injury for the clinical cardiologist. *Circulation AHA,* Retrieved from http://circ.ahajournals.org/content/105/20/2332

Yan, L. e. a. (2009). Autophagy in ischemic preconditioning and hibernating myocardium . *Taylor & Francis Group,*

Yang, S. e. a. (2010a). Rapamycin protects heart from ischemia/reperfusion injury independent of autophagy by activating PI3 kinase-akt pathway and mitochondria KATP channel. Retrieved from http://www.ingentaconnect.com/contentone/govi/pharmaz/2010/00000065/00000010/art00010?crawler=true

Yang, S. e. a. (2010b). Rapamycin protects heart from ischemia/reperfusion injury independent of autophagy by activating PI3 kinase-akt pathway and mitochondria KATP channel. *Pharmazie*, , 760-765. Retrieved from https://www.ingentaconnect.com/contentone/govi/pharmaz/2010/00000065/00000010/art00010?crawler=true

1. Zhang, S. e. a. (2013). *Cell autophagy and myocardial ischemia/reperfusion injury*. China: Intech.10.5772/53442

APPENDIX

If there is more than one appendix, label by letter (Appendix A, Appendix B, etc.). Appendix material may be single-spaced and of a different font than the rest of the thesis. Use Normal for a single-spaced style, or copy and paste from other sources.